Renewable and Sustainable Energy Reviews 74 (2017) 1147–1169

Contents lists available at ScienceDirect

Renewable and Sustainable Energy Reviews

journal homepage: www.elsevier.com/locate/rser

A new MPPT scheme based on a novel fuzzy approach

M. Nabipour*, M. Razaz, S.GH Seifossadat, S.S. Mortazavi

Department of Electrical Engineering, Faculty of Engineering, Shahid Chamran University of Ahvaz, Ahvaz, Iran

ARTICLE INFO

Keywords:
MPPT
PV
Membership functions tuning
Adaptive
Fuzzy controller

ABSTRACT

In this paper, after defining Maximum Power Point Tracking (MPPT) control expectations, with the aim of finding the optimum routine in fulfilling these expectations, a review over the available MPPT control methods is presented. Throughout the review, by comparing conventional MPPT routines in terms of accomplishing defined control objectives, the necessity of designing a new MPPT control scheme based on adaptive fuzzy logic is expressed. Based on the conducted review, a new routine to optimize the MPPT performance of a Photovoltaic (PV)-setup and to fulfill all the MPPT control requirements is proposed. The optimization is performed in tracking the Maximum Power Point (MPP) of the PV-module by a Boost-converter using an "antecedent-consequent adaptive" indirect fuzzy-based MPPT scheme. The fuzzy-based scheme is tuned online using a novel computationally light membership function tuning routine, where the antecedent and consequent membership functions are tuned synchronously. As a result, a fast, smooth and computationally light MPPT controller is proposed. In this regard, the presented MPPT scheme tuned using the proposed novel tuning routine is compared with conventional direct and indirect fuzzy-based MPPT schemes, showing superiority of the proposed MPPT routine over conventional schemes.

1. Introduction

With continuously growing concerns about fossil fuels and their effects on environments, the attentions are attracted to renewable energy sources as replacements. Among different types of renewable energies, because of easy implementation, low maintenance and constantly dropping PV-module prices, the solar energy has been considered as a suitable replacement for conventional energy sources. As a result, PV plants have been utilized globally in various regions [1].

Despite all merits and advances in PV technology, higher initial investment cost is imposed to the consumers compared to its conventional fossil fuel counterpart [1]. Moreover, highly nonlinear characteristics of PV-arrays caused by dependence of PV-modules to the surrounding ambient conditions have limited the global utilization of solar energy. To overcome these drawbacks, two solutions have been presented by the researchers. Improving the silicon semiconductors employed in the PV-modules has been considered as the first solution. Therefore, new semiconductors were tested which improved the performance of PV-setups. Yet, the improved modules were available at a very high price limiting the utilization of such modules to certain fields such as space and military studies [2].

In the other solution presented by the researchers improving the performance of PV-modules in tracking the MPP, is considered. The main goal in MPPT is operating the PV-setup at a point where the highest efficiency level possible is obtained. In this regard, various routines were implemented to track the MPP where Perturb and Observe (P & O) [3], incremental conductance (IC) [4] and Hill Climbing (HC) [5] could be counted as the most common conventional MPPT routines. Easy implementation and high reliability in nominal cases could be outlined as advantages of these routines. Yet, performance of the mentioned schemes deviate from desirable expectations when operating in realistic environmental conditions consisting of sudden variations in irradiance and temperature levels. As a result of these deviations, power oscillations and losses increase, resulting in lower system efficiency [6].

On the other hand, it has been acknowledged that the Artificial Intelligence (AI) approaches express superior performance compared to conventional MPPT methods, in terms of speed, accuracy and efficiency [7].

Considering drawbacks of conventional MPPT schemes, nonlinear and time variant nature of MPPT tasks, recent advances in implementation of AI methods due to recent trends in micro controller technology and superior performance of AI methods, AI schemes have been considered as a reliable alternative for conventional MPPT methods [9]. In fact, the desire to utilize AI lies in the approach that is intended to build applications that possess some intelligence, or

* Corresponding author.
E-mail addresses: m-nabipour@phdstu.scu.ac.ir (M. Nabipour), razaz_m@scu.ac.ir (M. Razaz), Seifossadat@yahoo.com (S.G. Seifossadat), mortazavi_s@scu.ac.ir (S.S. Mortazavi).

http://dx.doi.org/10.1016/j.rser.2017.02.054
Received 31 October 2016; Received in revised form 20 January 2017; Accepted 12 February 2017
Available online 17 March 2017
1364-0321/

Nomenclature

V_s	Boost Input Voltage
I_s	Boost Input Current
V_o	Boost Output Voltage
I_o	Boost Output Current
D_{b1}	Disturbances Affecting The Boost Current
D_{b2}	Disturbances Affecting The Boost Output Voltage
L	Inductor
R_L	Inductor Resistance
C	Output Capacitor
R_C	Output Resistive Load
m_i	The System Degree
n	The Number of Inputs
X_i	The Ith Input State Variable
${x_i}^{m_i}$	M_i^{th} Degree Time Derivative of The Ith Variable
$A_i(\underline{x}_i)$	Continuous State Function
$b_i(\underline{x}_i)$	Control Gain
y_i	Plant Output
$u_i \in R$	The Control Input
$P_i(\underline{x}, x^{m_i})$	The Outside Disturbances
$\underline{e}_i$	Ith Variable's Error Vector
$\underline{y}_{d_i}$	Desired Output Trajectory's Vector
$\underline{y}_i$	Actual Output Trajectory's Vector
M	Number Of Rules
$\widetilde{F}_i^j$	Antecedent Membership Functions Of X_i
θ^j	Centroids Of The Output Membership Functions
$\mu_{\widetilde{F}_i^j}$	Membership Grade Of X_i Related To $\widetilde{F}_i^j$
Y	Fuzzy Output
$P(N)$	Nth Sampling Time's Output Power Of The P(I) Curve
$I(N)$	Nth Sampling Time's Output Current Of The P(I) Curve
D	Duty Cycle
S	Solar Irradiance Level

more precisely, seem to be intelligent. This approach became very popular with the development of expert systems about thirty years ago. AI may be used to provide innovative ways of solving design issues and will allow designers to get an almost instantaneous expert opinion on the effect of a proposed change in a design [10,11]. In this regard various AI methods such as Neural Networks (NN) [12], Fuzzy Logic (FL) [13] and Genetic Algorithm (GA) [14,15] have been successfully implemented in various fields. Among the mentioned schemes, neural based and fuzzy logic based approaches can be considered as the most common AI approaches in the field of MPPT [15,16].

Neural networks have been implemented in various MPPT studies [17–19]. In case of a comprehensive and extensive training routine, based on a large set of data, which is generally time-consuming and complex to process, if the plant under control remains unchanged, the implemented NN method will perform satisfactorily without prior knowledge of plant parameters [9].

Despite acceptable implementations, NN applications are bounded by its structural limitations. These limitations are mainly caused by the nature of the pre-implementation approach utilized to train the NN. In this regard, the following drawbacks have been pointed out in various researches:

Using a very complex and time consuming training routine, usually prior to controller implementation, the NNs are trained to emulate the behavior of the specific under control plant. This is generally achieved by utilization of a sufficiently large set of historical input-output data. To ensure reliable operation of the NNs in a specific environment, the relation between the nodes and different layers (the applied weights) must be carefully and accurately determined by the applied training routine. Hence, the PV module is tested for a long period (months or even years) so that the suitable input and the output relation of the NNs are obtained [7,9]. In this regard, the time-consuming nature of the training process is one of the main drawbacks of the neural-based schemes [20,21].

Moreover, as mentioned in [22–25], neural networks are still considered as unstable learning model regarding to the presence of noisy sets, large training set, underfitting and overfitting problems that causes a lack of generalization and trapping on local minima solutions.

These drawbacks make the NN a less attractive approach of control in practical and real-time implementations in environments where uncertainties and disturbances are constantly changing the model of the plant and input-output relations under control.

The FLC on the other hand has presented promising results under varying conditions and perturbful, nonlinear and complex environments where the unknown plant model experiences variations through time [26–28]. Simple linguistic terms, simple structure, easy implementation, capability to regulate complex nonlinear plants with unknown mathematical model and the ability to estimate various nonlinear functions are among the advantages leading to widespread utilization of FL in various fields [7,9,29]. The fuzzy logic has also been widely utilized in the field of optimizing the power consumption of solar arrays [30–33]. In this regard, compared to other AI methods such as NN, in case of proper tuning, the FL scheme has proven to exhibit superior performance in terms of efficiency and dynamic response [15].

Despite promising results presented in various researches [7,9,26–33], dependency of the FL performance to the expert's knowledge could be counted as the main drawback of this approach. As a result, in the conventional type of this controller where the fuzzy parameters are not properly tuned, mainly due to the forms utilized in designing the membership functions and the rule-base, performance deviations from optimal expectations in environments with uncertainties are observed [34].

To overcome the effect of environmental conditions on controller performance, minimize the need for designers experience, reduce the rule-base size and improve the performance of fuzzy controllers, some efforts were made to tune the membership functions of the Fuzzy Logic Control (FLC) scheme [29,35]. In some researches, offline tuning of the membership functions were suggested. These offline routines consisted of heavy algorithms such as neural networks or even genetic-based algorithms which required a notable time taking training regime to perform suitably [36]. Using the offline processes to tune some of the parameters made these routines unsuitable for real-time applications and limited their implementations only to theoretical cases [37]. Moreover, it could be noted that in most of these documents, unrealistic assumptions such as considering the control gain, denoted by "b_i", as a known function [37], or as an undefined function with known sign [38] or even as an unknown constant [39], will also limit the applicability of the fuzzy logic to theoretical studies [40]. On the other hand, in most of the online adaptive schemes only one set of membership functions (i.e. consequents) are tuned. In this regard, it will be shown that while tuning the antecedent and consequent membership functions of a fuzzy- based scheme improves the overall system dynamics and steady states behavior, limiting the tuning process only to one set of membership functions (i.e. antecedent or consequent membership functions), limits the controller's capabilities. Therefore, schemes which tuned all the membership functions online, were focused on by researchers [40–42].

Moreover, many of the online methods tune the membership functions based on heavy algorithms, increasing the overall system's calculation burden [40–42]. Implementing such routines requires stronger ICs, where in such cases, the need for a stronger IC increases the overall system cost. In this field of study, it can easily be seen that

no serious research regarding tuning approaches to tune the antecedent and consequent membership functions of an indirect fuzzy controller, online, using a simple algorithm without using unrealistic assumptions has been reported.

Due to the importance of choosing a suitable MPPT algorithm, a review on available MPPT schemes is presented as the first contribution in this paper. In the majority of the reviews dedicated to this field of operation, the authors tend to examine the performance of various controllers with different natures. After presenting characteristics of these controllers, the superior controller is determined. For example, in [7–9], different classic MPPT approaches are compared with AI MPPT schemes. Moreover, in [15], various AI methods are compared in terms of various control indexes. Yet, no considerable review has been conducted in which, apart from efforts to compare different classical and AI approaches, the performance of sub-branches corresponding to adaptation routines in MPPT controls and fulfilling design objectives are examined. Moreover, comparing different forms of FLC consisting of direct classic FL and adaptive fuzzy, especially in terms of adaptive (online or even offline) characteristics in tracking the MPP has never been performed before. In this regard, examining the available MPPT control methods throughout the presented review to find the optimum control approach in terms of capabilities to fulfill the defined MPPT objectives, and proposing the optimum control routine characteristics has been considered as the main contribution and objective in this paper. On this basis, the efforts were put in obtaining the optimum MPPT control characteristics through answering the following questions throughout the review process:

1. Are the common classical MPPT routines, despite simple implementations and low cost, good choices to track the MPP desirably in terms of dynamic speed, steady states smoothness and efficiency?
2. Despite high accuracy, do all the AI methods exhibit desirable MPPT performance in terms of various control indexes?
3. Is the classic fuzzy approach, with simple implementation characteristics, an optimum approach to track the MPP at all instances?
4. Can impeccable MPPT performance be expected from FL control with a slight increase in the computational load caused by tuning only the consequent membership functions?
5. Can optimum MPP tracking behavior with computationally light characteristics be expected from available membership functions tuning routines which tune the antecedent and consequent membership functions online?

On this basis, a review in three levels is presented in this paper. In the first level, conventional MPPT algorithms, consisting of classic and soft computing MPPT methods are compared. After expressing general characteristics of various conventional methods, AI approaches with the potential to fulfill determined design objectives were selected as superior methods compared to classical MPPT methods. Then, by presenting characteristics of different AI methods, advantages and drawbacks of each scheme is determined; as a result, the FL was chosen as the advantageous and reliable MPPT approach among the AI methods. In the third level of the review, due to incapability of the classical fuzzy logic in fulfilling design goals at the same time and improvement of the performance of the FL in case of desirable parameter tunings, various FL tuning and adaptation methods are examined and presented. After examining the characteristics of various adaptation methods, by focusing on online adaptation methods, the drawbacks of these methods are pointed out and because of the complexity and costly nature the reported tuning approaches where all the membership functions are simultaneously adapted, the necessity to improve the adaptation process is expressed.

To minimize the mentioned drawbacks, a novel MPPT controller is presented as the second contribution of this paper. This MPPT controller, consists of a fuzzy-based MPPT scheme tuned using a proposed novel membership function tuning routine; where unlike [39], [37] and [38], "b" is considered to be a "time varying", "unknown function" with "unknown sign and magnitude" respectively.

The proposed tuning routine adapts the MPPT control loops to the present environmental conditions. It also synchronously tunes the antecedent and consequent membership functions online using a simple algorithm, where it will be shown in the simulations section that tuning both the antecedent and consequent membership functions improves the performance of the controllers notably. The resultant controller is a robust, computationally light, online tuned FLC-based scheme where all the membership functions are tuned synchronously.

To exhibit the applicability of the proposed controller, simulation results using the MATLAB-SIMULINK environment are presented. In the field of MPPT and current reference tracking, the proposed method is compared with conventional direct and adaptive indirect fuzzy controllers [37] to see the best tracking performance in following the desired power and current trajectory. The results exhibit the superiority of the proposed controller over conventional fuzzy and linear controllers in terms of dynamic and steady states performances.

This paper is described as follows. In Section 1, the introduction is given and the main problem dealt with in this paper is described. Where in Section 2 the literature review regarding the topic of MPPT control is presented. The literature review is then followed by PV setup and modeling in Section 3. The problem formulation and the proposed approaches are respectively given in Sections 4 and 5; where in Section 6 the simulation results are presented. Finally in Section 7 the conclusion is given.

2. Previous MPPT control works

In utilizing the solar energy, various factors are effective in optimizing the efficiency of PV modules. The efficiency of the structure of the PV module (9–17%) which are compared in Table 1, operational efficiency of the utilized inverter (95–98%) and the efficiency of the control structure to extract power from the PV module (higher than 98%) are among the most important factors [43,44]. In this regard, due to impossibility of changing the structure of the PV after installations, modifying the MPPT controller is considered as the simplest method to improve the performance of the PV module. On this basis, due to the importance of the quality of MPPT control, objective control requirements are expressed as fast dynamics, smooth steady states performance, high efficiency, high reliability logical calculation complexity and design cost. In this regard, different MPPT approaches were presented and their ability to fulfill expressed control requirements was examined.in literature to improve the performance of PV setups. These approaches can be categorized in three main branches such as offline, online and hybrid [45].

Offline MPPT approaches consist of methods where generating the proper control signal to track the MPP is only achieved through utilization of structural variables such as PV cell's short circuit current, temperature, irradiance level and open circuit voltage [47–49]. In this regard, low accuracy and efficiency are considered as the mutual drawback of such approaches.

On the other hand, the online methods, without the need for any specific offline training procedures attempt to generate the desired control signal based on real-time PV output parameters. P & O [50], IC [51] HC [52] are assumed as the most important classical online MPPT methods.

Table 1
PV structure dependent efficiencies [46].

c-Si based		Thin Film		
Sc-Si	mc-Si	a-Si,Si/μc-Si	CdTe	CIS/CIGS
14–20%	13–15%	6–9%	9–11%	10–12%

In [50], Kota has utilized P & O method to track the MPP. In this research, they have initially examined the performance of the classical P & O method in tracking the MPP and have determined the advantages and drawbacks of this type of MPPT control. In this research, it has been said that despite easy implementation, the classical P & O method presents undesirable behavior in MPPT tasks. In this regard, steady states power oscillations, undesirable dynamic performance and low efficiency could be counted as the shortcomings of such MPPT methods. To overcome such characteristics, in [50] a tangent based P & O routine is proposed. Based on the performed simulations, improvements in the performance of the MPPT scheme are confirmed.

IC is the other classical MPPT controller which was examined in [51] and implemented on a PV setup. In this research, similar to [50], the authors initially attempt to examine the characteristics of conventional IC control schemes in tracking the MPP. After determining the drawbacks, similar to the ones exhibited by the P & O scheme, the constant step size is recognized to be the main cause of these drawbacks. Hence, in the presented solution, variable step size is utilized instead of a fix step size. This modification in the nature of the step size results in considerable improvements in the MPP tracking performance compared to the classical MPPT routines. In this regard, increase in the efficiency, diminishing the steady states ripples and improvements in the dynamic response are observed as a result of this controller modification. This fact is confirmed in [51] using the performed simulation and the practical implementation results.

As the last classical MPPT algorithm, an example of successful HC implementation is given in [52] by Loukriz et al. in this research, the authors initially attempt to obtain a model for the PV cell. Following the PV model determinations, considering general classical MPPT method drawbacks, a new converter referred to as the SEPIC converter is presented. By implementing the HC algorithm on the PV cell using the mentioned converter the MPP is properly tracked. The desirable performance of the HC routine in combination with the proposed converter is conformed using the simulations results.

The third branch in MPPT control is hybrid approach which is constructed by combining characteristics of the online and offline MPPT approaches. In the category, by combining a usually offline pre-implementation training routine and online process of real-time data, the suitable control signal to track the MPP is generated. This type of MPPT approach generally consists of optimization algorithms such as PSO [52–55] and GA [14,56,57] and artificial intelligence methods such as FL [37,57–61], NN [62–65].

Among the mentioned AI methods, only the FL and the NN can be directly implemented, while GA and PSO algorithms are usually utilized to tune other processes. In this regard, some applications of the optimization algorithms are presented in [52–57].

In [53] Miyatake et al. have benefited from the PSO algorithm to control multiple-PV modules. The authors by confirming the complexity of controlling multiple-PV modules using classical MPPT techniques, have proposed a novel PSO-based algorithm. In this algorithm, using a multi objective function and by minimizing the installed sensors the MPPT of the PV module is successfully controlled in various operational conditions.

In [54], the PSO routine is utilized to improve the MPPT control performance by Shaque et al. in this research, the main MPPT control routine is selected to be HC and hence, the PSO is utilized to optimize the performance of the classical HC algorithm and directly generate the required converter duty cycle. Following this optimization, the resultant HC algorithm is then compared with conventional classic MPPT algorithms where the improvements are clearly observed.

In [55] Renaudineau et al. by refereeing to the capabilities of the PSO algorithm compared to other optimization routines corresponding to simplicity of implementation, higher convergence speed and independency to the initialization point, have utilized the PSO algorithm to improve the MPPT performance. In this regard, the MPPT task was considered for a PV setup consisting of multiple series connected PV modules connected to a high voltage BUS. To reach the optimum operation point in terms of the power extracted from the whole setup, the MPPT problem was treated as a multi-objective optimization problem. In this regard, the mentioned problem was optimized by the PSO considering the relations between the output components of the PV module such as the PV current and voltage.

In [56] Yang et al. Have benefited from the capability of the GA in finding a global optimum point to tune the structure of a hybrid solar-wind setup. In this research, the authors have used the GA to increase the systems reliability and optimize the performance of the system at cases where the energy source is lost. In this regard, in the optimum design procedure, various objectives such as the systems reliability in all instances and the annual installation cost are considered. To solve such a problem, variables such as the number and direction of the solar cell, the number of batteries and the wind turbines and the height of the wind turbines were optimized by the GA.

Also in [57], the GA was again utilized to optimize the performance of a base controller in tracking the MPP. The utilized base controller is a FL controller applied to a PV module feeding a simple load. In this work, after comparing the performance of the conventional FL controller with classical P & O MPPT controller, the stages of optimizing the fuzzy controller were discussed. Following the optimization, the resultant GA-optimized FL scheme was compared with other discussed schemes in tracking the MPP during various environmental conditions. The results relate to the superiority of the genetic-based optimized FL scheme over conventional and traditional routine.

As the last example of successful implementation of GA in MPPT tasks, the research presented by Daraban et al. in [14] was examined. In [14], the GA is utilized to optimize the P & O algorithm in tracking the global MPP at conditions where multiple local MPP exist. By using the P & O inside the genetic algorithm, the authors have managed to decrease the calculation load of the optimization process along with improving the performance of the P & O in tracking the global MPP. Independency to initial settings and capability to be implemented on a wide range of PV modules is considered as the characteristics of the proposed scheme.

FL on the other hand has also been successfully implemented to track the MPP. FL implementation in case of proper tuning presents fast dynamics, moth steady states behavior and independency to plant model and high robustness and efficiency. In this regard, in [58] Panda et al. have attempted to implement the classic form of the FL to track the MPP of a specific PV setup. In this work, the fuzzy rules are constructed based on operational principles of the classic P & O routine. Based on the output variables of the PV module such as the output current, voltage and the extracted active power, the fuzzy output is constructed and is directly fed to the DC-DC converter as the desired duty cycle to track the MPP. In fact utilizing the FL to directly generate the control input is referred to as the direct fuzzy approach which will be described later in this section.

At the end, by comparing the MPPT performance of the conventional direct fuzzy with the classical P & O approach, the superiority of this routine with respect to various control indexes is demonstrated. Similar studies were also conducted in [59] where equivalent results were obtained.

Another application of the indirect fuzzy MPPT control is demonstrated in [60] by Chiu et al. In this study two new solutions are proposed as MPPT controllers. Both of the proposed solutions are simultaneously implemented and compared. The first solution is referred to as the maximum power-voltage based routine. In this routine, after receiving the PV current, voltage and power signals, the reference PV output voltage corresponding to the MPP is generated. The generated reference voltage is then fed to the FL controller in charge of generation of the duty cycle. In this case, the objective of the FL controller is to minimize the error between the PV output voltage and the generated reference voltage.

In the second solution, as the output PV signals are received, the

controller attempts to minimize the slope of the P-V diagram by varying the output voltage of the PV module. It could easily be confirmed that as the operation point approaches the MPP, the magnitude of the P-V slope decreases; where in the case where the operation point is located directly on the MPP, the magnitude of the slope is minimized to zero. To evaluate such MPPT solutions, practical implementations have been performed, where the resultant improved MPP tracking performance is clearly observed.

Another application of fuzzy control is presented in [61] by El Khateb et al. in this study the FLC is used to generate the duty cycles of the combination of a SEPIC converter and an AC inverter. On this basis, in this study two individual FL controllers are utilized. Tracking the MPP by proper DC converter duty cycle generation is defined as the main objective of the first FL controller, while in the second FL controller, generation of a suitable load voltage is considered as the main objective. In this regard, by sensing PV output parameters, the reference output voltage to track the MPP is generated. This reference voltage is then fed to the first FL controller and the suitable control output to regulate the SEPIC converter is generated. The SEPIC's output voltage feeds the DC-link coupled to the inverter, where by proper inverter control, the demanded AC voltage is generated. As a result of such systems, apart from improvements in the MPP performances, the THD of the AC system is also reduced.

In the other form of implementation of the FL, referred to as the indirect fuzzy approach, the control input is not directly generated by the FL scheme. In fact, in this type of application, the FL is used to tune, adapt and improve the performance of another controller. In this regard, in [37] this branch of applications of FL is examined. In this study, the MPP is tracked using two levels of control loops. In the first loop, the physical position of the PV is determined in a way so that the maximum amount of irradiance possible is received. Following the optimization of the PV position, a fuzzy adaptive P & O routine is utilized to track the MPP. In this type of application, the FL tunes the P & O parameters online based on real-time PV output parameter data. On this basis, the desired PV output voltage corresponding to the MPP is generated by the P & O algorithm. The P & O output is hence directly fed to a linear PI controller, acting as the duty cycle regulator, so that the desired duty cycle to track the MPP is generated. Having the desired duty cycle generated by the PI controller, it is applied to the DC-DC converter using simple PWM methods. At the end, the validity of this approach is confirmed using simulations and practical implementations.

NN is also an attractive approach of control in which a model of a specific plant is generated through a comprehensive training process. In [62], a NN scheme is utilized to track the MPP corresponding to a PV module installed to feed a solar vehicle. In this regard, similar to the fuzzy approach presented in [60], output voltage generation consists of two stages. Initially, by training the NN offline, using an adequately large set of experimental PV input-output data, the relation between the environmental conditions and the reference output voltage corresponding to the MPP is obtained. As a result, for every combination of environmental parameters, a reference voltage to maximize the PV output power is derived. This reference voltage is then fed to a linear duty cycle controller, where the objective of the controller is to minimize the error magnitude between the reference and the actual PV output voltages. Finally, the authors have confirmed that by using such solutions, the number of sensors required for practical implementation is reduced and the MPPT efficiency is improved.

Following the research presented in [62] Ocran et al. have presented a different method of PV modeling and MPP tracking by utilizing NN [63]. In this study, with a DC motor as the load, similar to the approach utilized in [62], initially an accurate model of the PV is obtained by training the NN using a sufficiently large set of training data. On this basis, for each combination of the environmental temperature and irradiance, the current and voltage corresponding to the related MPP are obtained. Using the obtained current and voltages, the authors attempted to calculate the corresponding maximum power. The resultant maximum possible power is then fed to the linear duty cycle regulator, where the efforts are put into minimizing the error magnitude between the actual and the reference output powers generated by the NN scheme. In similar research conducted in [64], similar performance was expected from the NN.

following the researches performed to implement NN, a novel approach is presented in [65]. In this study, instead of utilizing the NN to model the plant as a whole and to determine the optimum voltage or power, a multi-layer NN is proposed to estimate nonlinear functions of the dynamic equations. In this regard, by accurately estimating the state functions using offline training data, state-feedback based schemes are utilized to minimize state errors. Considering the mentioned discussions, characteristics of various AI MPPT methods are given in Tables 2–4.

In various researches, comparisons between the classical and AI MPPT algorithms are performed. In these reviews, drawbacks such as slow dynamics, high steady states oscillations and low efficiency were reported as classical MPPT control characteristics. Hence, it is easily concluded that the classical MPPT methods fail to fulfill the control requirements and therefore cannot be considered as the optimum control approach. On the other hand, advantages of AI methods in terms of higher efficiency, lower steady states oscillations, higher tracking speed and reliability are confirmed. In this regard to examine the performance of different MPPT schemes, in [8] by Mellit et al., a comprehensive review and comparison of different MPPT approaches is presented. In this review, after listing various MPPT approaches, the authors have presented a comprehensive categorization based on pre-implementation and during implementation requirements. On this basis, the MPPT schemes are categorized into offline, online and hybrid schemes. Following this categorization, from each branch a control method is selected and compared with other present MPPT routines in terms of dynamic speed, efficiency and implementation simplicity. Where as a result of this comparison, superiority of the AI methods in terms of dynamic speed, tracking efficiency and steady states oscillations over conventional classic MPPT schemes is proven.

Table 2
Optimization Based MPPT Routines.

	Authors	Year	Application
PSO Based Optimization	MIYATAKE et al.	2008	Search for global MPP with reduced number of sensors
	Kashif Ishaque et al.	2012	Tune HC-Control MPPT using a Buck-Boost Converter
	Letting et al.	2012	Act as a C-Mex S-function to tune FLC rules
	Renaudineau et al.	2014	Optimization of operation point of multiple-PV modules connected in series attached to a high voltage BUS to achieve MPPT
Genetic Based Optimization	Yang et al.	2008	Optimal structure defining of a hybrid wind-solar setup
	Larbes et al.	2009	Tune the FLC to improve MPPT performance
	Daraban et al.	2014	Tune the P & O to improve MPPT performance
	Lasheen et al.	2016	Tune the PI controller to improve MPPT performance

Table 3
Classical Fuzzy Logic based MPPT control.

Authors	Year	Control Variable	Converter Type	Controller Type	Application
Panda et al.	2011	DC-Converter Duty Cycle	Buck-Boost	Direct	The desired Voltage is generated by P & O and fed to the FL by which the duty cycle is generated
Chiu et al.	2011	Duty Cycle	Buck	Direct	FL is implemented for MPV based routine and direct maximum power control.
Khateb et al.	2012	DC-Converter Duty Cycle and AC inverter switching signals	Sepic and AC inverter	Direct	Double FL is utilized to generate duty cycle of the SEPIC converter with the reference voltage being generated by the P & O algorithm. An AC inverter is also switched using the second converter.
Nabulsi et al.	2012	P & O parameters	Buck	Indirect	FL is used to tune P & O in tracking the MPP
Bendib et al.	2014	DC-Converter Duty Cycle	Buck-Boost	Direct	The desired Voltage is generated by P & O and fed to the FL by which the duty cycle is generated

Following the research given in [8], another comprehensive comparison of various MPPT schemes is given in [46]. Similar to the review given in [8], routine categorization is also performed in [46], where based on experimental results, superiority of the AI methods over classical MPPT schemes is confirmed. Moreover, the authors have also listed the future work expectations on renewable energy sources. In this regard, by grouping the different aspects and requirements for implementation of the MPPT schemes to branches such as control module, Fault-detection and diagnosis module, Monitoring and supervision module and Prediction module, application of AI in improving the operation of each module is demonstrated.

In [66] a thorough examination is presented and different MPPT schemes are analyzed from different aspects. After expressing general characteristics of different approaches, the authors have divided the MPPT schemes to two branches of classical and soft computing MPPT methods. On this basis, all the sub-branches of each category are then compared through pre-determined criteria. At the end, by presenting the advantages and disadvantages of each scheme, the authors have confirmed the superiority of the soft computing or AI methods over conventional classic MPPT techniques.

In this regard, a comparative study on both AI and conventional MPPT methods has been performed by Mellit and Kalogirou in [67]. In this research, various MPPT techniques were implemented, tested and compared under different conditions. In this review, based on various simulation results, the authors have confirmed that by utilizing AI methods, the dynamic and convergence speeds increase, control performance and efficiency are improved and steady states oscillations are decreased. Moreover, possible divergences in variable weather conditions are minimized. Similar results have been reported in other researches such as [7,9]. Moreover, considering the above characteristics, a brief comparison over the general MPPT schemes is given in Table 5.

Corresponding to the comparisons made in Tables 5 and 6 and reference [7,68], the AI routines are considered as the superior approaches. In this regard, due to optimizing nature of GA and PSO algorithms, only FL and NN methods can be considered as direct control approaches. To determine the suitable AI approach in fulfilling control requirements, numerous researches have been conducted based on comparison of these two approaches.

To ease the process of choosing between the NN and FL to perform MPPT tasks, extensive comparison between the FL and the NN have been presented in [15,16]. In these researches, the FL is assumed to be properly tuned and the NN is also considered to be well trained using an adequately large set of data.

In [15], the FL and NN controllers are applied to track the MPP throughout the experimental validations. The utilized PV module consists of two parallel Siemens SM50-H 50w arrays feeding a 24 V load. In this research, the comparison between the FL and the NN is based on practical evaluations. In this regard, the FL and the NN are respectively tuned and trained using data gathered from the operating system. Based on the experimental results, the authors have proven that by applying the FL, the MPP is followed with lower error, higher accuracy and increased output power compared to the NNs.

In the review given by Chekired et al. in [16], various FL and NN schemes such as randomly tuned FL, desirably offline tuned FL, ANN and ANFIS were compared. These schemes were subjected to various environmental variations such as constant variations in irradiance and temperature, rapid variations of irradiance and rapid variations of temperature. In all the mentioned cases, the desirably tuned FL exhibited superior performance compared to other AI schemes including the ANN. This performance improvement has been evaluated using various control indexes such as higher efficiency, higher response speed and lower steady states oscillations compared to the NN method. The results of these simulations were also confirmed by experimental results. Hence, judging based on the mentioned NN and fuzzy characteristics as their drawbacks and merits, and the conclusions given in [15,16], the FL can be considered as a reliable AI choice in tracking the MPP. The results of these comparisons are also presented in Tables 7 and 8 [15,16,69].

Despite desirable dynamics and steady states behavior and high efficiency when properly trained, due to the complex training routine required by the NN approach, parameter dependence of this approach and impossibility to generalize a pre-tuned NN to control multiple environments, based on findings given in [69], the NN approach cannot be considered as a reliable MPPT method. Moreover, the overall cost of designing and implementing an NN scheme due to the large set of data and complex algorithms is generally high. Hence, the NN fails to fulfill all the control requirements at the same time. On the other hand, Since the NN is trained to control a specific plant in a particular environment, it is considered to be a heavily environmental dependent solution. In this regard, when implemented as an MPPT controller, in case of any changes in the structure of the PV module, the training

Table 4
NN-based MPPT control.

Authors	Year	Control Variable	Converter Type	Modeled Plant	Application
OCRAN et al.	2005	MPP Voltage	Boost	PV-Module	The PV structure is modeled by NN and the reference MPP voltage is generated
Bahgat et al.	2005	MPP Power	Buck	PV-Module	The PV structure is modeled by NN and the reference MPP Power is generated
Ramaprabha1 et al.	2009	MPP Power	Boost	PV-Module	The PV structure is modeled by NN and the reference MPP Power is generated
Lin et al.	2011	MPP Voltage	Boost	PV-Module	The PV structure is modeled by NN and the reference MPP Power is generated
Kassem	2012	State Functions	Buck-Boost	State Functions	Multi-level NN is utilized to estimate state functions used in feedback linearization approaches

Table 5
AI and classical MPPT control characteristics [68].

	Classical MPPT Control			AI MPPT Control			
Method	**P & O**	**IC**	**HC**	**GA**	**PSO**	**NN**	**Classic FL**
Advantages	• Simple construction • Easy implementation • Less sensor requirements	• Highly efficient for steady change in irradiance • Simple and highly reliable	• Easy construction • Most proficient algorithm in slow irradiance changes	• wide search possible • can be applicable to fast changes in irradiance	• Effective usage of search space • Highly effective in search for global maximum • Simple and reliable • Highly effective in handling nonlinearities	• Effective for all types of irradiation conditions • Accuracy in solutions	• Highly robust • Accurate error detection • Very effective when combined with other AI methods
Method	**P & O**	**IC**	**HC**	**GA**	**PSO**	**NN**	**Classic FL**
Disadvantages	• High perturbation rate • High oscillations around MPP	• Power frequency oscillations • Poor convergence	• Less capable in handling dynamic changes in irradiance • Useful only in low power applications	• High memory requirements • Large computation process • Time consuming training routines	• Initializations of parameters are difficult • Computation is difficult in large populations	• High computational time • High memory requirements • Heavy training required • High plant and Environment dependence • Low reliability when uncertainties are present	• Hard to converge with fast irradiance variations • Rules cannot be changed once defined

procedures are to be repeated. On the other hand, it has to be noted that the structure of PV arrays are time-variant. This means that the structure of a specific PV module experiences various changes over time. As a result, to ensure reliable performance of neural based schemes, periodical training procedures have to be considered, where in each training procedure a new set of significantly large set of training data is processed by a complex optimization algorithm. Besides variations in the structure of the PV module, some other common phenomena such as unforeseen weather conditions, unpredicted climate changes or even changes in the converter circuit caused by temperature variations force the training routine to be repeated again. It should also be noted that for real-time implementation of a neural-based scheme in practical environments where the system dynamics are constantly subjected to parameter variations, the number of periodic training procedures increase significantly to ensure reliable operation of the control scheme. Due to the computational complexity and time-consuming nature of the training process, for the scheme to be practically implementable for real-time applications, much stronger micro controllers with higher computation power must be utilized. Such micro controllers significantly increase the overall cost of the controller design [7,9,22–25].

Moreover, based on the results given in [69] corresponding to the superiority of the well-tuned FLC over fully trained NN approaches in terms of tracking error, efficiency and output power, this logic is found to present potential of fulfilling all the control requirements at the same time and hence is considered as the main control logic to track the MPP in this paper.

Despite all the mentioned advantages and constructive characteristics, shortcomings such as dependency to expert knowledge have limited the application of fuzzy based MPPT schemes. To minimize this drawback, efforts have been made to tune the FL parameters [70–84]. In the initial form of these efforts, pre-implementation offline tuning using optimization algorithms such as the GA [70–76] and the PSO [77–85] are considered.

Tuning FL parameters using GA has been reported in various researches. For example, in [70], Messai has managed to optimize the fuzzy membership functions using GA. It is shown that by successful GA implementation and proper tuning of fuzzy parameters, the performance of the genetically tune FL exhibits notable improvements compared to the conventional FL controller. Apart from MPPT GA-FL has seen much attention in various fields [71–76]. In this regard, data mining [71,72], pixel classifications [73,74], time series forecast [75], mining fuzzy association rules [76], and etc... could be pointed out as GA-FL reported applications.

Apart from the GA, the PSO algorithm has also seen much attention in the field of fuzzy parameter optimizations in MPPT applications [77–81]. Other than in the MPPT control field, PSO-based fuzzy optimization has also been applied in the fields of robotics [82], grid frequency control [83], identification on smart phones [84], load frequency control [85] and etc....

Table 6
AI and classical MPPT control characteristics.

	Classical MPPT Control			AI MPPT Control			
Method	**P & O**	**IC**	**HC**	**GA**	**PSO**	**NN**	**Classic FL**
Tracking Speed	Low	Low	Low	High	High	High	High
Convergence Speed	Low	Low	Low	High	High	High	High
Complexity	Low	Low	Low	High	High	High	Low
Implementation	Easy	Easy	Easy	Difficult	Moderate	Moderate	Moderate
PV Dependent	No	No	NA	No	No	Yes	No
Prior Training	No	No	No	Yes	Yes	Yes	Yes
Efficiency	Low	Moderate	Moderate	High	High	High	High

Table 7
Comparison of Fuzzy-based and Neural based schemes.

Controller	Complexity	Response Time	Efficiency	Required Sensors	Steady States Oscillations	Overall Cost
Optimally Tuned FL	Complex	Very fast	Most efficient	Current, Voltage	Negligible	Medium
Classic FL (No Tuning)	Simple	Fast	Efficient	Current, Voltage	Low	Medium
Optimally Trained NN	Complex	Fast	Efficient	Voltage, Temperature, Irradiance	Low	High
ANFIS	Complex	Fast	Efficient	Voltage, Temperature, Irradiance	Low	High

Table 8
Comparison of Fuzzy-based and Neural based schemes During Various Tests.

Controller	Fast Temperature variations		Fast Irradiance variations	
	Efficiency (%)	Response time (s)	Efficiency (%)	Response time (s)
Optimally Tuned FL	98.2	2.97	97	3.12
Classic FL (No Tuning)	98.07	8.23	96.4	8.15
Optimally Trained NN	97.86	7.75	96.66	7.84
ANFIS	97.52	7.87	96.25	7.92

Despite desirable operations in predetermined conditions, this type of tuning is considered to be an offline routine and will deviate from desirable operational characteristics when implemented to control real-time applications in environments where disturbances, nonlinearities and perturbations exist [37]. Thus, this is considered as the obstacle in the process of optimal performance of FL. As a result of these deviations, besides time consuming implementation process, the offline tuned FL fails to fulfill control requirements and hence, cannot be considered as the target optimum control method.

To reduce the sensitivity of the fuzzy controller to disturbances, nonlinearities and perturbations, efforts were made to adapt the structure of this logic online [37]. In this regard, this type of logic can be analyzed from two points of view. From the application point of view, the adaptive fuzzy logic is categorize into two branches namely direct and indirect adaptive fuzzy approaches. The difference between these two approaches is mainly due to the routine utilized to generate the control signal. In the direct FL approach, the output of the FL controller is directly applied to the plant as the control input. While in the indirect approach the FL is utilized to tune other control schemes [38]. The most important application of the adaptive indirect fuzzy approach is in estimating various nonlinear functions. In this type of application, the adaptive indirect fuzzy approach benefits from the global estimation theory. Based on the global estimation principles, the fuzzy logic can be utilized to estimate any nonlinear but bounded function on a compact set [86].

Apart from the application point of view, the fuzzy logic can also be categorized from the turning point of view to “consequent adaptive” and “antecedent-consequent adaptive” routines. The viewpoints of these two approaches coincide in the method used to tune the consequent membership functions. While the methods suggested to tune the antecedent membership functions are completely different. In the “consequent adaptive” approach the antecedent membership functions are tuned offline similar to methods used in [70–84] to tune the classic direct fuzzy approach [37,87–90].

Therefore, in [87] the fuzzy adaptive approach with adaptive consequent membership functions has been utilized to estimate various nonlinear state functions and control input gain. In this study, the authors benefit from hybrid adaptation laws to guarantee accuracy of estimations. In this type of adaptation, the modeling and tracking errors are utilized where the control efforts are made to minimize these errors. To evaluate the performance of the proposed scheme, it has been implemented on inverse pendulum and chaotic systems.in both cases desirable operations were observed and reported. In another attempt by Barkat et al., estimation of state functions using adaptive consequent fuzzy membership functions has been implemented in [37]. Robust control of the PMSM drive using desirable fuzzy-based state function estimations in tracking a reference speed trajectory has been presented as the main control objective in [37].

Moreover, successful control of the inverse pendulum and magnetic levitation using adaptive fuzzy-based function estimations has been reported in [88]. The fuzzy logic has directly been utilized in this study where the output of the FL is adapted using simple Lyapunov's theory formulations. In all the implemented methods, Large calculation load forced to the system by the tuning routine, time-consuming training procedure and dependency to training data and most important of all, the offline nature of the antecedent membership functions tuning procedures are considered as notable drawbacks of the “consequent adaptive” adaptation routines. Moreover, it will be shown that by utilization of adaptive output membership functions and stationary offline-tuned antecedent membership functions, the performance of the adaptive fuzzy logic experiences some limitations.as a result of these limitations, the adaptive fuzzy controller will deviate from desirable performance characteristics. And hence fails to fulfill these control requirements. These limitations are not observed while adapting the antecedent and consequent membership functions simultaneously, as proposed in the “antecedent-consequent adaptive” routine. As a result, the control performance is improved and the online adapted “antecedent-consequent” presented potentials to optimally fulfill the control requirements.

To minimize the time consumption, and dependency to the training data or even the designer's experience related to the pre-implementation training routine, various simultaneous adaptation routines were proposed by researchers in [40,41,91–94]. In the approach presented in [91], all the consequent and antecedent fuzzy membership functions are adapted and obtained online. In this research, by defining various objective functions with different weighing factors, using complex optimization algorithms, the antecedent membership functions are simultaneously tune with the consequent membership functions as the environmental conditions and the operation point change. Following the research presented in [91], in [41] simultaneous adaptation of fuzzy membership functions is done by limiting the possible membership function forms to specific pre-defined shapes. In these shapes, for each membership function three structural parameters are considered such as the center of the membership function, the left and the right point of the membership function. For each membership function, various possible combinations are constantly checked with an algorithm similar to PSO so that the optimum membership function shapes could be reached.

Another simultaneous tuning algorithm is presented in [40] by M.J. and Deng. in this work the simultaneous adaptation of the membership functions is achieved through implementation of a objective function based Q-learning approach. Similar to [41], the implemented algorithm is of optimization search type where by which a large calculation burden and a time-consuming heavy training procedure is forced to the control system.

Yu et al. have also presented a novel membership functions tuning routine in [94]. It is clearly observable that tuning the membership functions is achieved using complex and heavy algorithms in this

report. Moreover, the authors have pointed out that in the adaptation algorithm, the data are initially categorized using clustering methods. Following this categorization, using a heavy learning based approach with variable rate is utilized to adapt all the membership functions and modify fuzzy parameters.

Gradient based approaches have also been reported among common approaches utilized in various researches to tune and adapt the antecedent and consequent fuzzy membership functions at the same instants, online [92,93]. These methods, apart from exhibiting slow convergence speed, force a heavy calculation load to the system and are generally only implementable to systems where obtaining gradients of nonlinear functions is possible.

High complexity of the adaptation algorithms, high computational load and high design and implementation cost can be considered as the mutual drawback of these adaptation routines. It can easily be observed that none of the mentioned schemes in this section manage to fulfill the control requirements at the same time. The performance of the discussed methods in fulfilling control requirements can be listed as follows:

- Classical MPPT routines fail due to low dynamic speed, high steady states oscillations and low efficiency.
- The NN as an AI method also fails due to environmental dependent and time-consuming training routine leading to low reliability.
- GA and PSO cannot even be considered as direct control methods since they can only be used to optimize other controllers and processes.
- The classical FL also fails since it requires proper tuning to show desirable performance at all instances.
- Although “Consequent-adaptive” shows improved performance, but it also fails since it requires tuning the antecedent membership functions similar to the classical fuzzy approach.
- The present “Antecedent-Consequent” methods also fail due to very high training complexity leading to costly implementations.

To overcome these drawbacks and yield an MPPT control approach capable of fulfilling all the control requirements at the same time, in this paper a novel tuning routine and as a result, a novel controller in which the antecedent and consequent membership functions are simultaneously adapted online using a computationally light algorithm is proposed. Using the proposed scheme the nonlinear functions, disturbances, nonlinearities and perturbations are estimated and by generating the suitable control signal, with the steady states and dynamic performance improved, the stability of the system is guaranteed.

3. PV setup and MPPT modeling

In this section, the PV-setup model is examined. The utilized model is depicted in Fig. (1a) and described in [30]. The PV-cells, being dependent on the environmental conditions, exhibit nonlinear characteristics when subjected to ambient parameter variations. These nonlinear characteristics include the relations between the output voltages (V), output current (I) and the Output Active Power (P). In this regard, to benefit the most from this source of energy, the maximum power must be provided by the PV-cells, where the efficiency is maximized. The maximum power is generated at a point referred to as the Maximum Power Point (MPP). The MPPs and the MPP variations caused by changes in the environmental conditions are respectively determined by black dots and dashed line in Fig. (1a). In this figure, various solar irradiance levels are denoted by $_{Si}$, where $i=1, 2, 3$, where the corresponding MPP currents are also denoted as I_{MPPi}. In this regard, Fig. (1a) demonstrates gradual increase in irradiance levels denoted by $_{Si}$ and their effect on the MPP. In this figure the relation between irradiance levels are defined as $S_1 < S_2 < S_3$.

Moreover, the setup utilized to track these MPPs is also demonstrated in Fig. (1b). This setup consists of a PV-module and a Boost-converter to control the PV-module output power.

As depicted in Fig. (1b), a DC/DC converter (Boost-Converter) is utilized to obtain a smooth power trajectory and track the MPP by controlling the PV-array output current and hence, output power. Based on this figure, multiple steps have to be taken. Initially, the actual position of the Operation Point (OP) has to be determined. According to Fig. (1a), since the relations between the current and power of individual PV-arrays differ from one to another and even change from on environmental condition to the other, the OP cannot be determined based on mathematical relations. Hence, an online algorithm is utilized to achieve this task. In this algorithm, the present output power and current of the PV-array are compared with the same parameters sampled in the previous sampling time. Using these set of data, the present location of the OP is estimated.

Having determined the present OP, a reference MPPT current signal denoted as I_{MPP}^{*} is generated by the MPP generator. This current, will be modified in a manner so that it tends towards I_{MPP}, acting as the reference current for the Boost converter. As a result, I_{MPP}^{*} has to be drawn from the PV-Module so that the MPP is tracked. Considering the Boost converter positioned at the inner control loop, it must have much faster dynamics compared to the outer loop components such as the MPP generator. With fast enough Boost converter dynamics, MPP reference current (I_{MPP}^{*}) can easily be drawn from the PV-module. Therefore, without loss of generality, the transfer functions mapping the I_{MPP}^{*} to the Boost input current “I_s” can be approximated as $G_{boost}(s) = \frac{I_s}{I_{MPP}^{*}} \cong 1$. Hence, it is observed that any variations in the I_{MPP}^{*} results in variations of the PV-module's OP. As a result, accurate modifications of the I_{MPP}^{*} can lead to desirable MPPT behaviors where the OP is moved towards the MPPs depicted in Fig. (1a).

In this process, the I_{MPP}^{*} is generated using the flowchart given in Fig. (2a). This flowchart is easily transferred to a fuzzy-based function where it is used in the fuzzy-based MPP-generator. The membership functions and the rule-base related to this fuzzy-based MPP-generator are given in Fig. (2b) and Table 9 where the control principles and the control schematics are respectively depicted in Figs. (2c and d).

In Fig. (2c), the variations of the I_{MPP}^{*} based on the present PV-

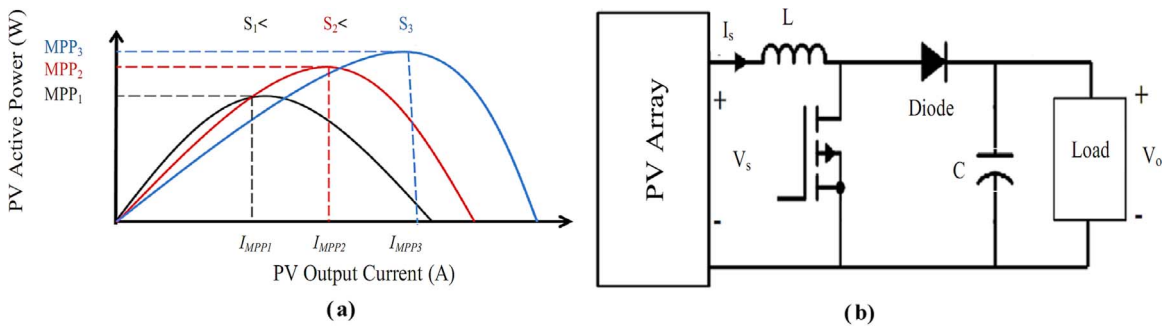

Fig. 1. PV-array output curves and operating setup, (a) PV Characteristics Curve (b) PV-Setup for MPPT.

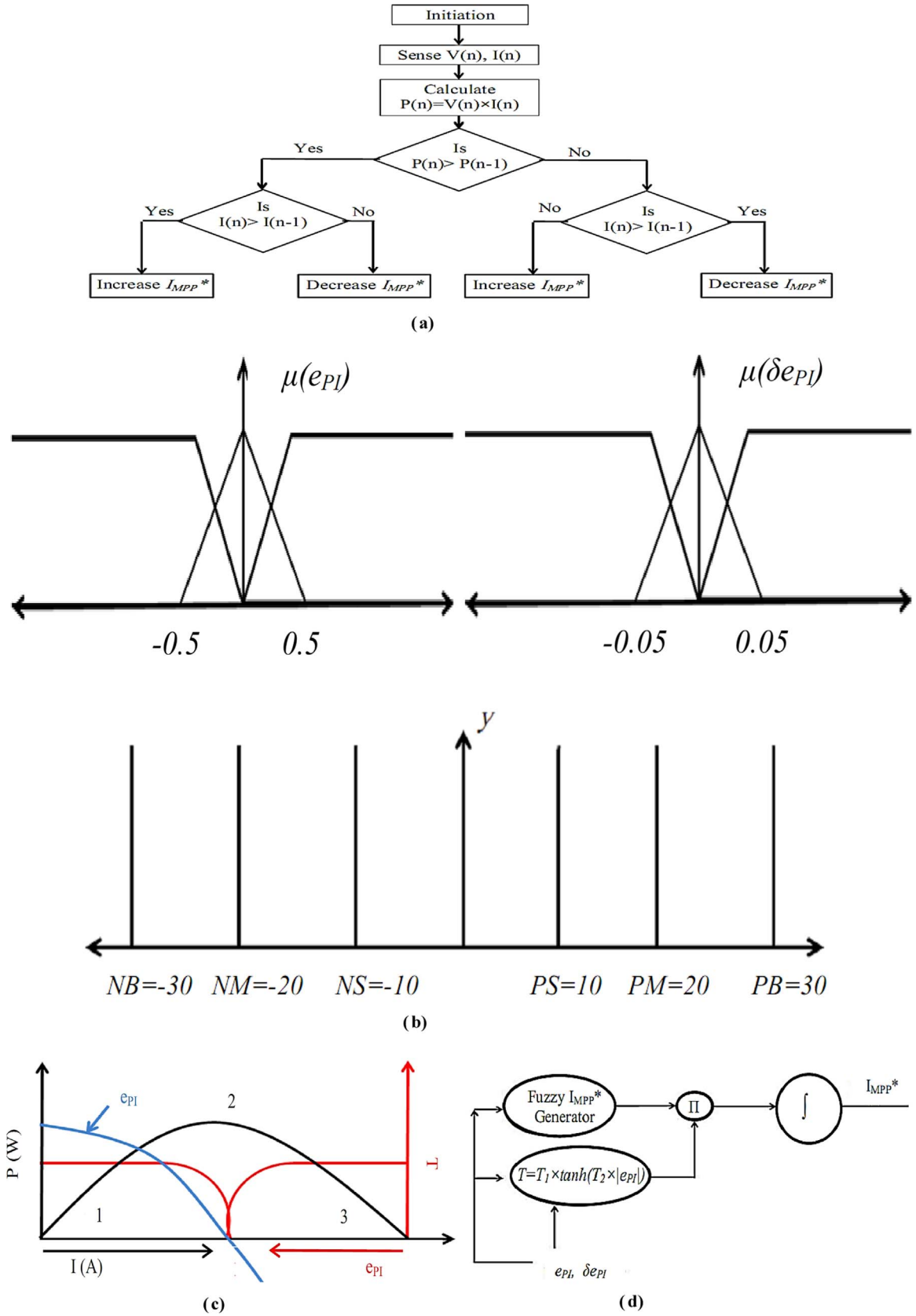

Fig. 2. I_{MPP}^{*} Generator (a) I_{MPP}^{*} Flowchart (b) I_{MPP}^{*} Generator Membership Functions (c) I_{MPP}^{*} and Adaptive Gain Principles, (d) Controller Schematics.

Table 9
Rule-base to generate the I_{PR} signal.

$e_{PI}/\delta e_{PI}$	N	Z	P
N	NB	NM	NS
Z	PS	Z	NS
P	PS	PM	PB

module's output is demonstrated, where:

$$e_{PI} = [P(n) - P(n-1)][I(n) - I(n-1)] \quad (1)$$

$$\delta e_{PI} = e_P(n) - e_P(n-1) \quad (2)$$

The principles of the MPP generation can easily be understood through Figs. (2b) and (c). As an example, for positive e_{PI} and δe_{PI}, it is inferred that the OP is approaching "1" from "2". Similarly for negative e_{PI} and δe_{PI}, the OP is approaching "3" from "2". Other cases are inferred in a similar manner. In fact, in all the possible variation in e_{PI}, δe_{PI} the present position of the OP is determined by the e_{PI} while the movement direction of OP is defined by δe_{PI} sign. Based on values of e_{PI}, δe_{PI} the required actions are taken by the $I_{MPP}{}^{*}$ generator using the scheme depicted in Fig. (2d). In this regard, the fuzzy-based controller, with the membership functions and rules, as depicted and presented in Fig. (2b) and Table 9 is utilized to control the $I_{MPP}{}^{*}$ as:

$$I_{MPP}{}^{*} = \int Y(e_{PI}, \delta e_{PI}) T \times dt \quad (3)$$

To overcome the common drawback observed in conventional direct fuzzy schemes, which is high frequency oscillations about the MPP, the adaptive gain "T" dynamics present in Fig. (2c) and is defined as follows:

$$T = T_1 \times tanh(T_2 \times |e_{PI}|) \quad (4)$$

where T_1 and T_2 are constants. Using this gain, as the OP tends towards the MPP, variations of $I_{MPP}{}^{*}$ will be limited. Thus, oscillations around the OP will be minimized. These oscillations in the drawn current result in severe ripples in the generated power by the PV-module, which in fact, damage the electrical instruments. In the simulations section, a comparison between the proposed schemes with the conventional direct fuzzy routine regarding the "active power" oscillations is presented.

Having the reference MPP current $I_{MPP}{}^{*}$ generated, it is fed to the Boost-Converter to be drawn from the PV-module. By accurate control of the Boost-Converter, $I_{MPP}{}^{*}$ will be tracked desirably and hence, desirable MPPT is guaranteed. In this regard, the Boost regulator plays a vital role in the MPPT procedure.

4. Problem statement

As mentioned in the previous section, desirable MPPT operation is highly dependent on the BOOST current regulator. The proposed control scheme is designed to regulate the BOOST current so that by tracking $I_{MPP}{}^{*}$ desirably, the MPPT task is achieved properly. Hence, in this section the general control problem dealt with in designing an MPPT controller, where the proposed adaptive fuzzy-based scheme used to control the Boost-Converter is discussed. In this regard, the Boost control dynamics are given as:

$$\dot{I}_s = \frac{1}{L}(-R + V_s - V_o(1-D)) + d_{B1} \quad (5)$$

$$\dot{V}_O = \frac{1}{C}((1-D)I_s - I_o) + d_{B2} \quad (6)$$

System dynamics given in (5) and (6) can clearly be treated as the Multi-Input Multi-Output (MIMO) system dynamic equations given in (7). Hence, in this research, the general control input for MIMO systems are derived, and then it is adapted to fit the Boost converter system requirements.

$$\begin{aligned} x_i^{m_i} &= A_i(\underline{x}_i) + b_i(\underline{x}_i)u_i + P_i(\underline{x}, x_i^{m_i})_{i=1,\dots,n} \\ y_i &= x_i \end{aligned} \quad (7)$$

The main goals in designing the control input are to minimize the tracking error and to guarantee plant's stability. In this regard, depending on the assumptions considered, the controller design can be treated in two ways, the ideal and the realistic approaches. In this section, the ideal approach is discussed while the realistic approach is treated in the next section.

A. Ideal approach:

In the Ideal approach, $A_i(\underline{x}_i)$ and $b_i(\underline{x}_i)$ are considered to be measurable and $P_i(\underline{x}, x_i^{m_i})$ is neglected. In this regard, considering $x = [x_1, x_2, \dots, x_n]^T \in R^n$, $\underline{x}_i = [x_i, \dot{x}_i, \dots, x_i^{(m_i-1)}]^T \in R^{m_i}$ and $\underline{x} = [\underline{x}_1, \underline{x}_2, \dots, \underline{x}_n]^T \in R^{n \times m_i}$, $\underline{e}_i$, $\underline{y}_i$ and $\underline{y}_{d_i}$ are formulated as:

$$\underline{y}_i = [y_i, \dot{y}_i, \dots, y_i^{(m_i-1)}]^T \in R^{m_i} \quad (8)$$

$$\underline{y}_{d_i} = [y_{di}, \dot{y}_{di}, \dots, y_{di}^{(m_i-1)}]^T \in R^{m_i} \quad (9)$$

$$\underline{e}_i = \underline{y}_{d_i} - \underline{y}_i = [e_i, \dot{e}_i, \dots, e_i^{(m_i-1)}]^T \in R^{m_i} \quad (10)$$

using (7)–(10), $\underline{e}_i$ dynamics are obtained as:

$$\begin{aligned} \dot{\underline{e}}_i &= F_i \underline{e}_i + G_i e_i^{m_i} = F_i \underline{e}_i + G_i(y_{di}^{(m_i)} - A_i(\underline{x}_i) - b_i(\underline{x}_i)u_i - P_i(\underline{x}, x^{m_i}) \\ e_i &= C_i^T \underline{e}_i \end{aligned} \quad (11)$$

where:

$$F_i = \begin{bmatrix} 0 & 1 & 0 & \cdots & \cdots & 0 \\ 0 & 0 & 1 & 0 & \cdots & 0 \\ \vdots & \vdots & 0 & \ddots & \ddots & \vdots \\ \vdots & \vdots & \vdots & \ddots & \ddots & 0 \\ 0 & 0 & 0 & \cdots & 0 & 1 \\ 0 & 0 & \cdots & \cdots & \cdots & 0 \end{bmatrix} G_i = \begin{bmatrix} 0 \\ 0 \\ 1 \end{bmatrix} C_i = \begin{bmatrix} 1 \\ \vdots \\ 0 \\ 0 \end{bmatrix} \quad (12)$$

By considering v_i as $v_i = y_{di}^{(m_i)} + K_i^T \underline{e}_i$, (5) is modified as:

$$\begin{aligned} \dot{\underline{e}}_i &= F_i \underline{e}_i + G_i e_i^{m_i} = F_i \underline{e}_i + G_i(v_i - K_i^T \underline{e}_i - A_i(\underline{x}_i) - b_i(\underline{x}_i)u_i - P_i(\underline{x}, x^{m_i}) \\ &= (F_i - G_i K_i^T)\underline{e}_i + G_i(v_i - A_i(\underline{x}_i) - b_i(\underline{x}_i)u_i - P_i(\underline{x}, x^{m_i}) \end{aligned} \quad (13)$$

$$e_i = C_i^T \underline{e}_i \quad (14)$$

where $K_i^T = [K_{i,1}, K_{i,2}, \dots, K_{i,m_i}] \in R^{m_i}$ are selected in a manner so that $(F_i - G_i K_i^T)$ is stable.

In the ideal approach, considering the ideal problem assumptions, where $A_i(\underline{x}_i)$ and $B_i(\underline{x}_i)$ are considered to be measurable and $P_i(\underline{x}, x_i^{m_i})$ is neglected, applying the control output u_{ideal} as $u_{ideal} = \frac{1}{b_i}(v_i - A_i(\underline{x}_i))$, the following is concluded:

$$\begin{aligned} \dot{\underline{e}}_i &= (F_i - G_i K_i^T)\underline{e}_i + G_i(v_i - A_i(\underline{x}_i) - b_i(\underline{x}_i)(\tfrac{1}{b_i}(v_i - F_i(\underline{x}_i))) \\ &= (F_i - G_i K_i^T)\underline{e}_i \end{aligned} \quad (15)$$

hence:

$$e_i^{(m_i)} + k_{i,m_i} e_i^{(m_i-1)} + \dots + k_{i,1} e_i = 0 \quad (16)$$

Thus, according to (16), we will have $\lim_{t \to \infty} e_i(t) = 0$, and hence, the asymptotical stability of the ideal system can easily be concluded [95]. Yet, in practice, since accurate plant model is not available, $A_i(\underline{x}_i)$ and are generally immeasurable. Moreover, system interactions and disturbances denoted as $P_i(\underline{x}, x_i^{m_i})$ have to be accounted for due to various disturbances and uncertainties, making the ideal problem assumptions invalid for realistic applications.

To design a suitable control law, the plant model or the state-based functions have to be estimated and the disturbance terms, $P_i(\underline{x}, x_i^{m_i})$, have to be accounted for. This is achieved by the proposed adaptive indirect fuzzy-based scheme, tuned using a novel membership func-

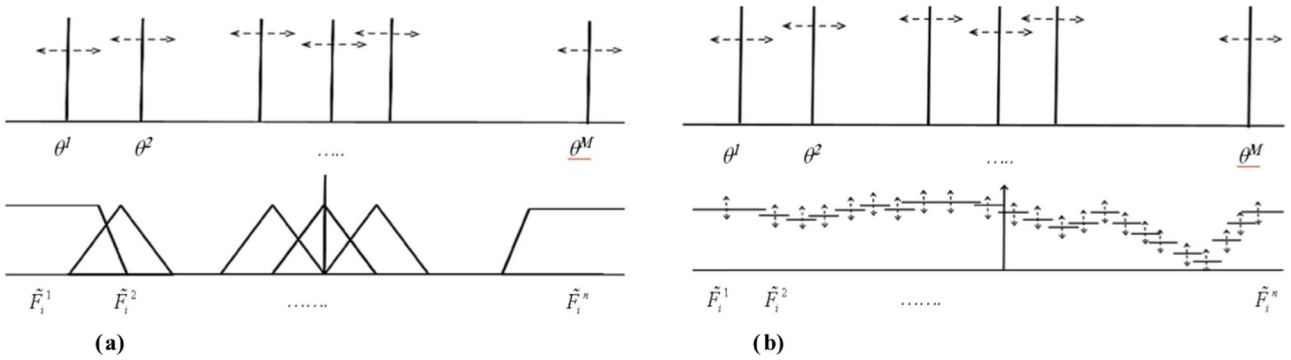

Fig. 3. Conventional and Proposed Fuzzy Parameter Tuning Routines (a) Conventional Tuning Routine of Fuzzy Parameters (b) Proposed Tuning Routine of Fuzzy Parameters.

tions tuning routine. In the proposed algorithm, all the fuzzy membership functions (i.e. the antecedent and consequent) are tuned synchronously using a simple routine, resulting in a controller with more degree of freedom and faster dynamics, compared to conventionally-tuned indirect fuzzy schemes and smoother steady states compared to conventional direct fuzzy controllers.

5. Proposed tuning routine and MPPT controller (realistic approach)

In the realistic approach, unlike the ideal form of the problem, the plant dynamic model and state-based functions $A_i(\underline{x}_i)$ and $b_i(x_i)$ are assumed to be immeasurable. Moreover $P_i(\underline{x}, x_i^{m_i})$, is also considered to be immeasurable. Hence, to design a suitable control law guaranteeing the desirable control goals (given later in this section), $A_i(\underline{x}_i)$, $b_i(\underline{x}_i)$ and $P_i(\underline{x}, x_i^{m_i})$ have to be estimated accurately. In this regard, the design process benefited from the principles of fuzzy logic approach, the global estimation theory and lyapunov's theory [96]. Based on these estimations, the desirable control law is generated.

Using the global estimation theory, which is the key aspect of indirect fuzzy approach, the fuzzy logic controller can be used to estimate any bounded function. The main structure of the fuzzy controller consists of the general **if-then** rules, presented as "$\boldsymbol{R^j} \equiv$ if $x_1 \in \widetilde{F}_1^j$ and $x_2 \in \widetilde{F}_2^j$ ...and $x_n \in \widetilde{F}_n^j$ then $y^j=\theta^j$, where $j=1,2,...,M$" and the inference process related to them. Hence, the output of the fuzzy controller is constructed as follows:

$$Y = \frac{\sum_{j=1}^{M} f^j \theta^j}{\sum_{j=1}^{M} f^j} = g \sum_{j=1}^{M} f^j \theta^j \tag{17}$$

where:

$$f^j = \prod_{i=1}^{n} \mu_{\widetilde{F}_i}{}^j,\ g = \frac{1}{\sum_{j=1}^{M} f^j} \tag{18}$$

The major contribution of the proposed design routine, besides the actions taken to estimate $b_i(\underline{x}_i)$, rests in the form considered for the membership functions. In the majority of the published documents regarding the online adaptation of the membership functions parameters, consequent membership functions are solely adapted [37]. In these types of tuning algorithms, only one parameter degree of modification, where only θ^j is modified, exists. Moreover the antecedent membership functions have to be tuned prior to controller implementation using heavy offline routines, where the calculation cost is directly proportional to the number of rules and input variables. A good example is tuning an indirect fuzzy controller for a plant with 6 inputs, and 3 antecedent membership functions dedicated to each input. To design such a system, 54 variables have to be tuned prior to the controller design. The parameters to be tuned rise to 63 for a system with 7 inputs. Moreover, the effect of antecedent membership function shapes (i.e. trapezoidal, triangular, Gaussian etc...) on the overall system behavior must also be considered. It could easily be concluded that various membership functions shapes affect different plant differently; hence, finding the optimum shape increases the design complexity.

To increase the degrees of dynamical freedom, improve the dynamic response of the indirect fuzzy approach, minimize the pre-implementation tuning efforts and find desirable membership functions shapes, online synchronous adaptation of antecedent and consequent membership functions is proposed in this research. In the presented approach the shape of the membership functions can be modified freely. It will be exhibited in the simulations section that, by using the proposed tuning algorithm, the dynamic and steady states responses of the controller improve significantly when compared to conventional adaptation routines. On the other hand, regardless of the number of rules, the number of the variables require tuning before implementation are limited to 3, minimizing the pre-implementation(offline) computation cost. Moreover, instead of heavy optimization routines utilized in [40–42], simple algorithms are utilized to tune the membership functions; hence, the online calculation burden is also decreased. Free shape adaptation could also be pointed out as one of the major superiorities of the proposed work over conventional tuning approaches. In this regard, the overall proposed membership functions tuning approach is depicted in Fig. 3. Further explanation corresponding to the adaptation laws and the tuning procedures are given in the subsequent sections.

In this approach, to tune the membership functions, the overall antecedent membership functions consist of n sub-membership functions. Each sub-membership function is modified online until the optimum shape is reached. In this regard, the tuning algorithms are explained in this section. Using the control law u_i, generated by the proposed indirect fuzzy approach, the state variables are moved towards or stay in a zone with small boundaries. In other words, the overall control system will be proven to be stable, asymptotically (i.e. $|\underline{x}_i| \le X_0$). Moreover, the tracking error is also moved towards or stays in a zone with small boundaries about zero (i.e. $|e_i| \le E_1$). Similarly, the reference output trajectory is proven to be tracked with minimum error (i.e. $|\underline{e}_i| \le E_0$). Finally, the final RMS values are proven to tend towards a zone with small boundaries (i.e. $RMS(e_i) \le R_0$ and $RMS(\hat{e}_i) \le R_1$). To reach the mentioned goals, the controller design assumptions are expressed as:

- **Controller design assumptions:**

(i) The state function $A_i(\underline{x}_i)$ and the perturbations function $P_i(\underline{x}, x^{m_i})$ are assumed to be unknown and immeasurable, but limited in a manner so that:

$$\sup_{t>0} |A_i(\underline{x}_i)| \le A_0 \tag{19}$$

and

$$\sup_{t>0} |P_i(\underline{x}, x_i^{m_i})| \le P_0 \tag{20}$$

(ii) Similarly, the control gain $b_i(\underline{x}_i)$ is assumed to be unknown and immeasurable in terms of magnitude and sign. This assumption is in direct contrast with the simplifying assumptions made regarding the variation nature [37,39] or even the sign of the control gain [38], made in great share of researches discussing indirect fuzzy approaches.

(iii) The reference output vector components, $\underline{y}_{d_i} = [y_{di}, \dot{y}_{di}, \ldots, y_{id}^{(m_i-1)}]^T \in R^{m_i}$, are assumed to be bounded as $\|\underline{y}_{d_i}\| \le Y_0$ and $\|y_{di}^{(mi)}\| \le Y_1$.

(iv) The fuzzy logic output *"Y"* can be used to estimate any unknown function denoted as *"H"* on a bounded set in a manner so that: $\|H - Y\| \le \xi$ [96]. In this regard, the actual state function is defined as:

$$A_i(\bar{x}_i) = W_i^{*T}(\bar{x}_i)\theta^*{}_i(\bar{x}_i) + \gamma_i^*(\bar{x}_i) = \sum_{j=1}^{M} g^* f^*{}_i^j(\bar{x}_i) \times \theta^*{}_i^j(\bar{x}_i) + \gamma_i^*(\bar{x}_i) \tag{21}$$

$$g^* = \frac{1}{\sum_{j=1}^{M} f^*{}_i^j} \tag{22}$$

where:

$$W^*{}_i^T = [W^*{}_i^1(\underline{x}_i), \ldots W^*{}_i^M(\underline{x}_i)] = g^*[f^*{}_i^1 \ldots f^*{}_i^M] \tag{23}$$

$$\theta_i^T = [\theta_i^1(\underline{x}_i), \ldots \theta_i^M(\underline{x}_i)] \tag{24}$$

Using assumption *iv,* estimated values of the state function are given as:

$$\widehat{A_i}(\underline{x}_i, \hat{\theta}_i) = \hat{W}_i^T(\underline{x}_i, \hat{\theta}_i)\hat{\theta}_i(\underline{x}_i) + \hat{\gamma}_i(\underline{x}_i) = \sum_{j=1}^{M} \hat{g}\hat{f}_i^j(\underline{x}_i, \hat{\theta}_i) \times \hat{\theta}_i^j(\underline{x}_i, \hat{\theta}_i) + \hat{\gamma}_i(\underline{x}_i) \tag{25}$$

$$\hat{g} = \frac{1}{\sum_{j=1}^{M} \hat{f}_i^j} \tag{26}$$

As a result, the estimated functions error is obtained as:

$$\widetilde{A}_i(\bar{x}_i, \hat{\theta}_i) = A_i(\bar{x}_i) - \widehat{A}_i(\bar{x}_i, \hat{\theta}_i) \tag{27}$$

where

$$\widetilde{A}_i(\bar{x}_i, \hat{\theta}_i) = \sum_{j=1}^{M} g^* f^*{}_i^j(\bar{x}_i) \times \theta^*{}_i^j(\bar{x}_i) - \sum_{j=1}^{M} \hat{g}\hat{f}_i^j(\bar{x}_i, \hat{\theta}_i) \times \hat{\theta}_i^j(\bar{x}_i, \hat{\theta}_i) + \tilde{\gamma}_i(\bar{x}_i, \hat{\theta}_i) \tag{28}$$

Theory-1:

Regarding assumptions (*i-iv*) corresponding to designing a suitable control law for MIMO plants given in (6), by using the following control input, tuned using the proposed membership functions tuning routine and rules given in (31–38), the controller design goals are achieved:

$$u_i = \frac{1}{\hat{b}_i(\underline{x}_i)}[\hat{U}_i + U_{K,i}] \tag{29}$$

where:

$$\hat{U}_i = -g_i(\underline{x}_i)\sum \hat{f}_i^j(\underline{x}_i) \times \hat{\theta}_i^j(\underline{x}_i) + \varepsilon_f(\underline{x}_i)] - \hat{P}_i(\underline{x}, x^{m_i}) \tag{30}$$

$$U_{K,i} = K_i(\tau_i) + \Gamma_i \operatorname{sgn}(\tau_i) \tag{31}$$

Considering the error variables as $\tau_i = 2\underline{e}_i S_i G_i$, $\tilde{\gamma}_i = \gamma_i - \hat{\gamma}_i$, $\widetilde{P}_i = P_i - \hat{P}_i$, $\tilde{b}_i = b_i - \hat{b}_i$, the tuning rules are:

$$\dot{\hat{b}}_i(\underline{x}_i) = -\frac{\tau_i}{\eta_i[\hat{b}_i(\underline{x}_i)]}[v_i - \sum_{j=1}^{M} \hat{g}\hat{f}_i^j(\bar{x}_i, \hat{\theta}_i) \times \hat{\theta}_i^j(\bar{x}_i, \hat{\theta}_i) + \hat{\gamma}_i(\bar{x}_i) + \hat{P}_i] \tag{32}$$

$$\dot{\hat{P}}_i(\underline{\hat{x}}, \hat{x}^{m_i}) = -\frac{(\tau_i)}{\varepsilon_i} \tag{33}$$

$$\gamma_i = -\frac{(\tau_i)}{\vartheta_i} \tag{34}$$

$$\Delta_i = -5.5(\tau_i) + 4.5\operatorname{sgn}(\tau_i),\ \Delta'_i = -5.5(\tau_i) + 4.5\operatorname{sgn}[(\tau_i)\theta_i^j] \tag{35}$$

$$\dot{\alpha}_i = -\frac{\Delta_i}{2\beta_i} \tag{36}$$

$$\dot{\hat{\theta}}_i^j = -(\frac{\Delta_i}{\Delta'_i})(\frac{\alpha_i}{\beta_i})[\frac{\hat{f}_i^j}{\hat{f}_i^j w_i + 1}] \tag{37}$$

$$\dot{\hat{f}}_i^j = \frac{\Delta_i \hat{f}_i^j - 2\beta_i{}^2\dot{\hat{\theta}}_i^j}{2\alpha_i\beta_i} \tag{38}$$

Proof of Theorem:

To prove Theory-1 and achieve the controller design goals, the following lyapunov's candidate function is utilized:

$$V = \sum_{i=1}^{n} V_i \tag{39}$$

where:

$$V_i = \bar{e}_i^T S_i \bar{e}_i + \frac{1}{2}\sum_{j=1}^{M}(\alpha_i{}^j\widetilde{f}_i^j + \beta_i{}^j\tilde{\theta}_i^j)^2 + \frac{1}{2}\vartheta_i\tilde{\gamma}_i^2 + \frac{1}{2}\varepsilon_i\widetilde{P}_i^2 + \frac{1}{2}\eta_i\tilde{b}_i{}^2 = \bar{e}_i^T S_i \bar{e}_i + +\frac{1}{2}\vartheta_i\tilde{\gamma}_i^2 + \frac{1}{2}\varepsilon_i\widetilde{P}_i^2 + \frac{1}{2}\eta_i\tilde{b}_i{}^2 + \frac{1}{2}\sum_{j=1}^{M}[(\alpha_i{}^j\widetilde{f}_i^j)^2 + (\beta_i{}^j\tilde{\theta}_i^j)^2 + 2\alpha_i{}^j\widetilde{f}_i^j\beta_i{}^j\tilde{\theta}_i^j] \geq 0 \tag{40}$$

while $\alpha_i{}^j$ and $\beta_i{}^j$ are dynamic gains, defined to guarantee the overall system stability and S_i is the solution to the following equation:

$$S_i F_i + F_i^T S_i = -Q_i \tag{41}$$

where Q_i is a symmetrical positive definite matrix. Requirements regarding the solutions to (41) are given in [97]. By neglecting subscripts and superscripts to prevent overcrowding the formulations, the derivation of V_i is obtained as:

$$\dot{V}_i = \dot{\bar{e}}_i^T S_i \bar{e}_i + \bar{e}_i^T S_i \dot{\bar{e}}_i - \vartheta_i\tilde{\gamma}_i\dot{\hat{\gamma}}_i - \varepsilon_i\widetilde{P}_i\dot{\hat{P}}_i - \eta_i\tilde{b}_i\dot{\hat{b}}_i + \left\{\sum_{j=1}^{M}[2\dot{\alpha}\alpha\widetilde{f}^2 - 2\alpha^2\dot{f} \times \widetilde{f} + 2\dot{\beta}\beta\tilde{\theta}^2 - 2\beta^2\dot{\theta} \times \tilde{\theta} + 2\dot{\alpha}\beta \times \widetilde{f} \times \tilde{\theta} + 2\alpha\dot{\beta} \times \widetilde{f} \times \tilde{\theta} - 2\alpha\beta \times \dot{f} \times \tilde{\theta} - 2\alpha\beta \times \widetilde{f} \times \dot{\theta}]\right\} \tag{42}$$

Combining (12) and (28), it is concluded that:

$$\dot{\bar{e}}_i = F_i\bar{e}_i + G_i\{v_i - A_i - P_i - b_i(\frac{1}{\hat{b}_i})\{v_i - [\sum_{j=1}^{M}\hat{g}\hat{f}_i^j(\bar{x}_i, \hat{\theta}_i) \times \hat{\theta}_i^j(\bar{x}_i, \hat{\theta}_i)] + \hat{\gamma}_i(\bar{x}_i) + \hat{P}_i\} \tag{43}$$

thus:

$$\dot{V}_i = -\bar{e}_i^T Q_i \bar{e}_i + 2\bar{e}_i^T S_i G_i[v_i - A_i - P_i - b_i\left(\frac{1}{\hat{b}_i}\right)\{v_i - \sum_{j=1}^{M}\hat{g}\hat{f}_i^j(\bar{x}_i, \hat{\theta}_i) \times \hat{\theta}_i^j(\bar{x}_i, \hat{\theta}_i) + \hat{\gamma}_i(\bar{x}_i) + \hat{P}_i] + \sum_{j=1]}^{M}[\dot{\alpha}\alpha \times \widetilde{f}^2 - \alpha^2\dot{f} \times \widetilde{f} + \dot{\beta}\beta\tilde{\theta}^2 - \beta^2\dot{\theta} \times \tilde{\theta} + \dot{\alpha}\beta \times \widetilde{f} \times \tilde{\theta} + \alpha\dot{\beta}\widetilde{f}\,\tilde{\theta} - \alpha\beta\dot{f} \times \tilde{\theta} - \alpha\widetilde{\beta f} \times \dot{\theta}] - \vartheta_{i\tilde{\gamma}i}\dot{\gamma}_i - \varepsilon_i\widetilde{P}_i\dot{\hat{P}}_i - \eta_i\tilde{b}_i\dot{\hat{b}}_i \tag{44}$$

By defining a new variable as $L_i = v_i - \sum_{j=1}^{M}\hat{g}\hat{f}_i^j(\bar{x}_i, \hat{\theta}_i) \times \hat{\theta}_i^j(\bar{x}_i, \hat{\theta}_i) + \hat{\gamma}_i(\bar{x}_i) + \hat{P}_i$ (44) can be modified to:

$$\dot{\bar{e}}_i = F_i\bar{e}_i + G_i\{v_i - A_i - P_i - b_i(\frac{1}{\hat{b}_i})(L_i)\} \tag{45}$$

And hence:

$$\begin{aligned}\dot{V}_i = &-\bar{e}_i^T Q_i\bar{e}_i + 2\bar{e}_i^T S_i G_i[v_i - A_i - P_i - b_i(\frac{1}{\hat{b}_i})L_i]\\ &+ \sum_{j=1}^{M}[\dot{\alpha}\alpha\times\tilde{f}^2 - \alpha^2\dot{f}\times\tilde{f} + \dot{\beta}\beta\tilde{\theta}^2 - \beta^2\dot{\theta}\times\tilde{\theta} + \dot{\alpha}\beta\times\tilde{f}\times\tilde{\theta}\\ &+ \alpha\dot{\tilde{f}}\tilde{\theta} - \alpha\beta\dot{f}\times\tilde{\theta} - \alpha\beta\dot{\tilde{f}}\times\dot{\theta}]\\ &-\vartheta_i\tilde{\gamma}_i\hat{\gamma}_i - \varepsilon_i\tilde{P}_i\hat{P}_i - \eta_i\tilde{b}_i\hat{b}_i\end{aligned} \tag{46}$$

which can be modified to:

$$\begin{aligned}\dot{V}_i = &-\bar{e}_i^T Q_i\bar{e}_i + \tau_i[v_i - A_i - P_i - (\frac{\tilde{b}_i}{\hat{b}_i})L_i - L_i]\\ &+ \sum_{j=1}^{M}[\dot{\alpha}\alpha\times\tilde{f}^2 - \alpha^2\dot{f}\times\tilde{f} + \dot{\beta}\beta\tilde{\theta}^2 - \beta^2\dot{\theta}\times\tilde{\theta} + \dot{\alpha}\beta\times\tilde{f}\times\tilde{\theta}\\ &+ \alpha\dot{\tilde{f}}\tilde{\theta} - \alpha\beta\dot{f}\times\tilde{\theta} - \alpha\beta\dot{\tilde{f}}\times\dot{\theta}]\\ &-\vartheta_{i\tilde{\gamma}i\tilde{\gamma}i} - \varepsilon_i\tilde{P}_i\hat{P}_i - \eta_i\tilde{b}_i\dot{\hat{b}}_i\end{aligned} \tag{47}$$

$$\begin{aligned}=&-\bar{e}_i^T Q_i\bar{e}_i + \sum_{j=1}^{M}[\dot{\alpha}\alpha\times\tilde{f}^2 - \alpha^2\dot{f}\times\tilde{f} + \dot{\beta}\beta\tilde{\theta}^2 - \beta^2\dot{\theta}\times\tilde{\theta} + \dot{\alpha}\beta\times\tilde{f}\times\tilde{\theta}\\ &+ \alpha\dot{\tilde{f}}\tilde{\theta} - \alpha\beta\dot{f}\times\tilde{\theta} - \alpha\beta\dot{\tilde{f}}\times\dot{\theta}]\\ &-\tau_i\tilde{A}_i + \tilde{\gamma}_i(-\vartheta_i\hat{\gamma}_i - \tau_i) + \tilde{P}_i(-\varepsilon_i\hat{P}_i - \tau_i) + \tilde{b}_i(-\eta_i\dot{\hat{b}}_i - \tau_i\frac{L_i}{\hat{b}_i})\end{aligned} \tag{48}$$

Using Eqs. (29), (31)–(38), the following equation s concluded from (48):

$$\begin{aligned}\dot{V}_i = &-\bar{e}_i^T Q_i\bar{e}_i + \sum[\tilde{\theta}^2(2\dot{\beta}\beta) + \tilde{f}^2(2\dot{\alpha}\alpha) + \tilde{f}\,\tilde{\theta}(2\dot{\alpha}\beta + 2\alpha\dot{\beta} - g^*(\tau))\\ &+ \tilde{\theta}(-g^*(\tau)\hat{f} - 2\alpha\beta\dot{\hat{f}} - 2\beta^2\dot{\hat{\theta}})\\ &+\tilde{f}(-2\alpha^2\dot{\hat{f}} - 2\alpha\beta\dot{\hat{\theta}} - g^*(\tau)(\hat{f}w + 1)\hat{\theta})]\end{aligned} \tag{49}$$

The membership functions are defined in a way that for all $i > 0$ we could have $1 \le g_i, g_i^* \le 10$. Hence Eq. (49) could be approximated as:

$$\begin{aligned}\dot{V}_i \le &-\underline{e}_i^T Q_i\underline{e}_i - K_i|\tau_i| + \sum[\tilde{\theta}^2(2\dot{\beta}\beta) + \tilde{f}^2(2\dot{\alpha}\alpha) + \tilde{f}\,\tilde{\theta}(\Delta + 2\dot{\alpha}\beta + 2\alpha\dot{\beta})\\ &+ \tilde{\theta}(\Delta\hat{f} - 2\alpha\beta\dot{\hat{f}} - 2\beta^2\dot{\hat{\theta}}) + \tilde{f}(-2\alpha^2\dot{\hat{f}} - 2\alpha\beta\dot{\hat{\theta}} + \Delta'(\hat{f}w + 1))]\end{aligned} \tag{50}$$

where

$$\Delta = \begin{cases} -(\tau) & (\tau) \ge 0\\ -10(\tau) & (\tau) \le 0\end{cases},\ \Delta' = \begin{cases} -(\tau) & (\tau)\hat{\theta} \ge 0\\ -10(\tau) & (\tau)\hat{\theta} \le 0\end{cases} \tag{51}$$

Equivalently:

$$\begin{aligned}\Delta &= -5.5(\tau) + 4.5\,\mathrm{sgn}[(\tau)](\tau)\\ \Delta' &= -5.5(\tau) + 4.5\,\mathrm{sgn}[(\tau)\hat{\theta}](\tau)\end{aligned} \tag{52}$$

By substituting Eqs. (35)–(38) in (50), if β_i^j is selected to be a constant, it is logical to assume $\tilde{f}^2 << 1$ and hence $\tilde{F}^2(2\dot{\alpha}\alpha)$ could be neglected. As a result, we have:

$$\dot{V}_i \le \Gamma'_i + \sum[\tilde{F}^2(2\dot{\alpha}\alpha)] = -\underline{e}_i^T Q_i\underline{e}_i + V_d \tag{53}$$

where $V_d = -K_i|\tau_i| + \sum[\tilde{F}^2(2\dot{\alpha}\alpha)] \cong -K_i|\tau_i| < 0$.

Considering $-\underline{e}_i^T Q_i\underline{e}_i \le -\lambda_{\min}(Q_i)\|\underline{e}\|^2)$, with the minimum Eigen value denoted as $\lambda_{\min}(.)$, the following is easily concluded:

$$\dot{V}_i \le -\lambda_{\min}(Q_j)(\|\underline{e}\|^2) + V_d \le 0 \tag{54}$$

Considering (40) and (54) where it is found that $\{\forall\, i | v_i \ge 0 and \dot{v}_i < 0\}$, as described in [95], the overall system is proven to be asymptotically stable and $\lim_{t\to\infty} e_i(t) = 0$. Moreover, the following relations could also be concluded:

$$\dot{V}_i \le -K_v V_i + K_v V'_d \tag{55}$$

$$V_i(t) \le \max(V(0),\ V'_d) \tag{56}$$

where

$$K_v = \frac{\lambda_{\min}(Q_i)}{\lambda} \tag{57}$$

$$\lambda = \max[\lambda_{\max}(S_i)] \tag{58}$$

$$V'_d = K_v\sum\max(\alpha\tilde{f} + \beta\tilde{\theta}) + \frac{1}{2\eta_i}K_v\{\max[\tilde{\gamma}_i^2] + V_d \tag{59}$$

$$|\underline{e}| \le \sqrt{\frac{\max(V(0),\ V'_d)}{\lambda_{\min}(P_i)}} \tag{60}$$

$$|\underline{x}_i| \le |\underline{y}_d| + |\underline{e}| \le Y_0 + \sqrt{\frac{\max(V(0),\ V'_d)}{\lambda_{\min}(P_i)}} \tag{61}$$

$$\lim_{t\to\infty}(\lambda_{\min}(S)|e| \le \underline{e}^T S\underline{e}) \le V'_d \tag{62}$$

$$\lim_{t\to\infty}|e| \le \sqrt{\frac{V'_d}{\lambda_{\min}(S_i)}} \tag{63}$$

$$\lim_{t\to\infty}\int_0^t(|\underline{e}|^2)dt \le \frac{V_d}{\lambda_{\min}(Q_i)} \tag{64}$$

$$\Rightarrow RMS(e) = \lim_{t\to\infty}\left[\sqrt{\frac{1}{t}\int_0^t(|\underline{e}|^2)dt}\right] \le \sqrt{\frac{V_d}{\lambda_{\min}(Q_i)}} \tag{65}$$

As a result, the design goals are clearly proven. To summarize, the variables that could be modified to tighten the bounds surrounding various parameters are expressed in Table 10.

6. Simulations and modeling

To examine the applicability of the proposed scheme in closed loop control structures, especially MPPT tasks, some simulations were performed on the PV-module presented in Fig. (1b). In these simulations, the PV-module is an NE165U1 module introduced in [98,99]. The corresponding nonlinear characteristic curves are depicted in Figs. (4.a and .b). In this regard, the utilized Boost converter parameters are as $[R_L, L, C, R_C]$ =[0.01Ω,0.01 H, 10μF, 25Ω], In these simulations, the following state equations are utilized:

$$\dot{I}_s = \frac{1}{L}(-R_L + V_s - V_o(1 - D)) + d_{B1} \tag{66}$$

$$\dot{V}_O = \frac{1}{C}((1 - D)I_s - I_o) + d_{B2} \tag{67}$$

Assuming state vectors as $\underline{x} = [x] = [I_s]$, $\underline{e} = e = [y_d - y] = [I_{MPP}^* - I_s]$, regarding Eqs. (38) and (39), in order for the input current to follow the reference MPP current accurately, with the I_{MPP}^* generator and the MPPT controller defined as depicted in Fig. (4c), the following control law was applied to the converter as the duty cycle:

$$u = D = \frac{1}{b_i}(v + \hat{\Gamma}sgn(e) - w(I_s)\sum\hat{F}^j(I_s)\times\hat{\theta}^j(I_s) - \hat{\gamma}(I_s) - \hat{P}(I_s, \dot{I}_s) \tag{68}$$

Table 10
Influence of Variables on System Bounds.

	$\|\underline{e}_i\|$	$\|\underline{x}_i\|$	$\lim_{t\to\infty}(\|e\|)$	$RMS(e)$
Parameters to decrease	$\max(V(0),\ V'_d)$	$Y_0,\ \max(V(0),\ V'_d)$	V'_d	V'_d
Parameters to increase	$\lambda_{\min}(S_i)$	$\lambda_{\min}(S_i)$	$\lambda_{\min}(S_i)$	$\lambda_{\min}(Q_i)$

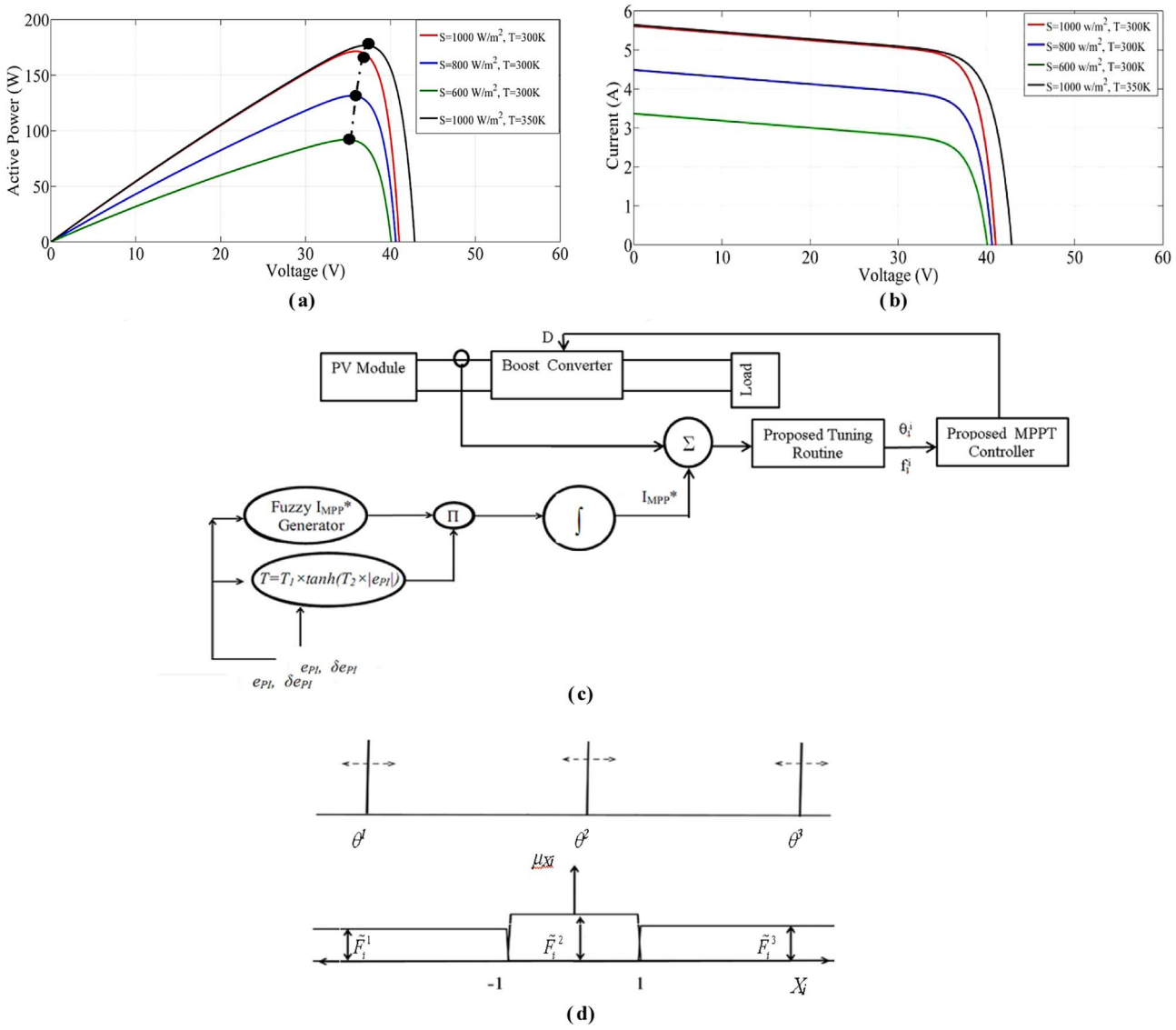

Fig. 4. : The Control Setup and PV Characteristic Curves (a) P-I characteristic curve of the utilized PV-module (b) I-V characteristic curve of the utilized PV-module (c) Control Setup (d) θ_i^j and f_i^j.

Table 11
Adaptive fuzzy rules of the proposed controller.

x_i	$x_i \in F_i^1$	$x_i \in F_i^2$	$x_i \in F_i^3$
Y_i	$Y_i = \theta_i^1$	$Y_i = \theta_i^2$	$Y_i = \theta_i^3$

where $v = 50000e + \dot{I}_{MPP}{}^*$, $\hat{\Gamma} = 1000$ and other parameters are determined based on (31)–(38). In the simulations performed, the fuzzy membership functions and rules presented in Fig. (4d) and Table 11 are employed. Moreover, without loss of generality, one could design the controller considering $\eta_i = \vartheta_i = \varepsilon_i = 0.01$.

The utilized membership functions for the proposed fuzzy-based scheme are presented in Fig. (4c). The height of the antecedent and horizontal position of the consequent membership functions vary based on Eqs. (34) and (36)–(38) to guarantee system stability or minimum tracking error.

In design and implementation of the proposed scheme some points must be considered. In this regard, when designing a conventional indirect fuzzy-based scheme, the antecedent membership functions are static. Due to these static membership functions, the membership degree of a specific state variable, at a certain magnitude, will always remain stationary. This membership degree is determined by the shape of the membership function, defined using structural parameters which are usually 3 for each membership function. Hence, by altering these structural parameters the membership degree of a specific state variable, at a certain magnitude could be modified. Moreover, since these membership degrees directly affect the output of fuzzy rules, their determination prior to controller implementation is of vital importance.

In conventional controller design procedures determining suitable membership functions, as mentioned in numerous occasions throughout this research is a time-consuming task with high calculation burden. On the other hand, in the proposed scheme, due to continuous adaptation of membership functions, when the corresponding rules are triggered, the membership degrees constantly adapt and tend towards optimum values. Hence, the initial structural parameter values will not have a significant effect on the performance of the overall control scheme. These functions along with the output centroids are adapted using Eqs. (32)–(38) based on the instantaneous values of the state variables.

Based on Eqs. (37) and (38), it is easily concluded that $\hat{\theta}_i^j$ and $\hat{f}_i^j$ remain constant when the fuzzy rule corresponding to f_i^j is not triggered. Meaning that $\hat{\theta}_i^j$ and $\hat{f}_i^j$ will adapt if and only if $\hat{f}_i^j$ possesses a non-zero magnitude. Hence, based on the proposed membership

function structure, depicted in Figs. (3b, 4d), it can easily be concluded that the maximum number of antecedent membership functions which are simultaneously modified is limited to 2 for each state variable. The rest of the antecedent membership functions are excluded from the adaptation procedure. This fact significantly reduces the control system's computation load compared to the schemes presented in [37], where all the membership functions must be monitored constantly.

Besides reduction in the online calculation cost, due to negligible effect of the initial settings of the proposed approach on the controller performance, the pre-implementation calculation effort can also be reduced using the proposed scheme. This is due to the dependence of the characteristics of the proposed scheme to only 3 parameters, namely η_i, α_i and β_i, while in the conventional indirect fuzzy approaches [37], the controller behavior is affected by 3 parameters for each membership function, namely the membership functions structural parameters. These parameters increase exponentially as the number of required rules increase; while for the proposed scheme, the number of variables with pre-implementation tuning requirements are constantly 3 at all conditions. This considerable reduction in pre-implementation calculation effort is another advantage of the proposed scheme over conventional methods.

In this section, five sets of simulations were performed. Initially, the behavior of the PV-module controlled using the proposed scheme are examined and the proposed MPPT algorithm is compared with conventional fuzzy-based MPPT scheme. In the second set, sinusoidal variations, in the third set "one day temperature and irradiance level" variations are compared using linear irradiance variation tests. In the 4th set of simulations, the proposed scheme is compared with the conventional indirect fuzzy controller in boost current tracking objectives. The last set of simulations tries to evaluate the generalization capability of the proposed scheme.in this set of tests the performance of the proposed scheme in tracking the MPP implemented on several types of multi-component or in other words Multi-Junction (MJ) PV models is examined.

T.1 Irradiance variations:

In this test, the purpose was to apply various possible linear irradiance trajectory variations to the PV-module. Hence, the irradi-

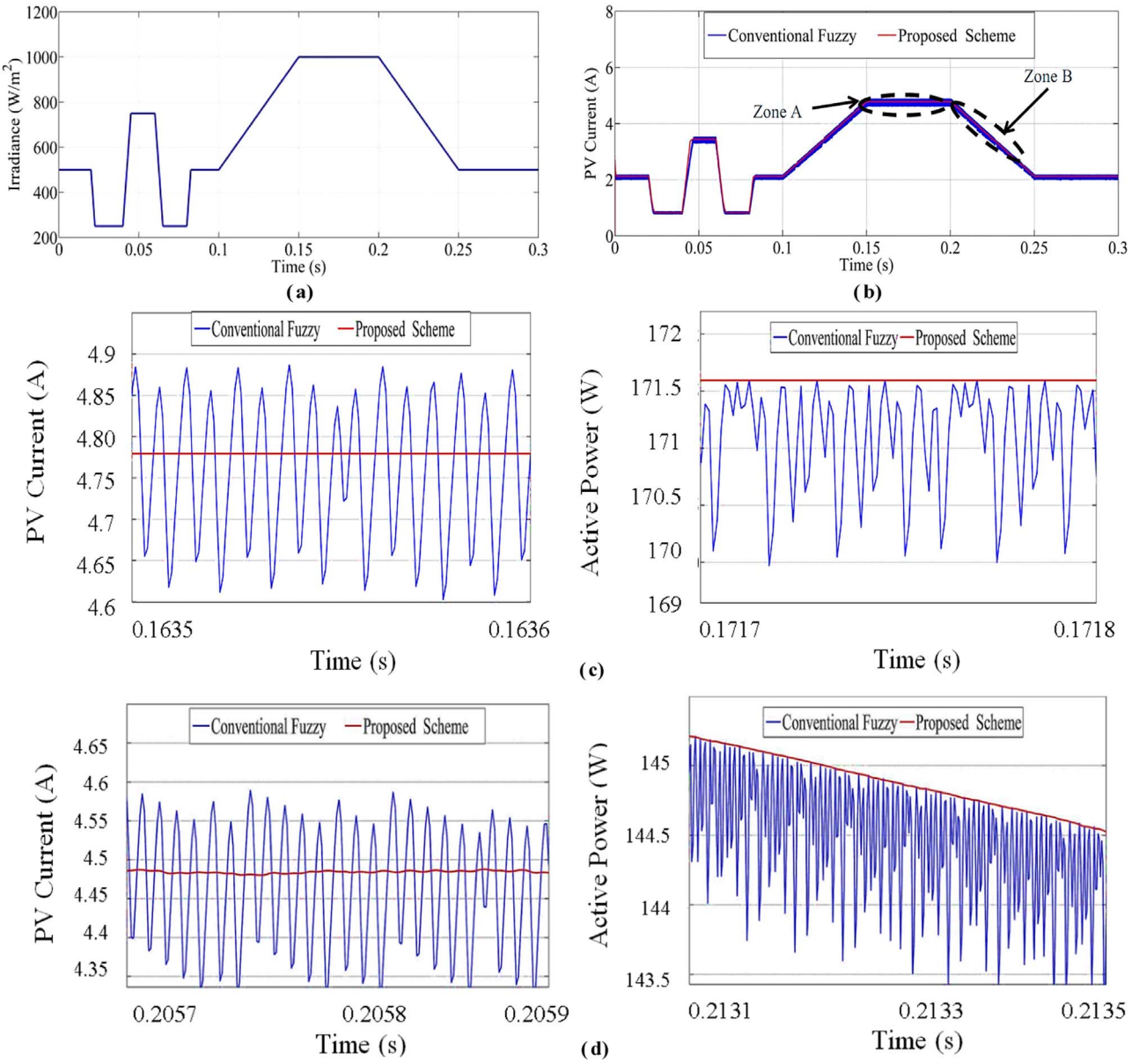

Fig. 5. Irradiation Variation Test (a): The Applied Irradiance Trajectory (b): Output Current of the PV-Module (c): Irradiance Variation Test Results Zone-A (d): Irradiance Variation Test Results Zone-B.

ance trajectory, depicted in Fig. (5.a) was applied to the PV-setup. Moreover, in Fig (5.b- d), the MPPT performance of the proposed scheme and the conventional direct fuzzy-based MPPT routines are demonstrated.

As depicted in Fig. (5a), at t=25 ms, after the OP of the PV-module has reached steady states, with a steep drop, the irradiance trajectory was set to S=250 W/m^2 form S=500 W/m^2. At t=40 ms, another step in the irradiance increased this level to S=750 W/m^2. Two more steep variations dropped and rose the irradiance levels at t=60 ms and t=80 ms, to S=250 W/m^2 and S=500 W/m^2 respectively. From this point forth, ramp variations were applied to the PV-module, raising the level to a maximum of S=1000 W/m^2 and returning it back to S=500 W/m^2. The initial ramp starts at t=100 ms and the second ramp initiated at t=200 ms. Using this type of variation, apart from dynamic behavior examinations, the steady states behaviors of the mentioned schemes are also examined.

Based on Fig. (5b), the initial Boost input current or in other words, the initial drawn current from the PV-arrays was Is=2 A. With the first drop, the current was decreased to about 1 A, and in the ramp starting at t=100 ms, reached 5 A. Throughout the irradiance variations, as demonstrated in Fig. (5b), the current was varied in the interval of [1 A, 5 A]. In Figs. (5c and d) the characteristic curves corresponding to zones A and B corresponding to both approaches are plotted respectively. Based on these figures, the oscillatory behavior of the conventional fuzzy-based MPPT schemes in tracking the I_{MPP}^{*} is clearly observable. This fact is also present in the "Active Power" plots depicted in Fig. (5c, d). On the other hand, the proposed scheme tracked the reference irradiance level with minimum error. Therefore, the drawn current followed the reference smoothly and the corresponding power followed the MPP at all instances.

T.2 Sinusoidal irradiance variation test:

In the next test, the irradiance trajectory is varied sinusoidally. The applied sinusoidal trajectory is demonstrated in Fig. (6a). The variations start at t=0.07 s with a magnitude equal to 250 W/m^2 increasing

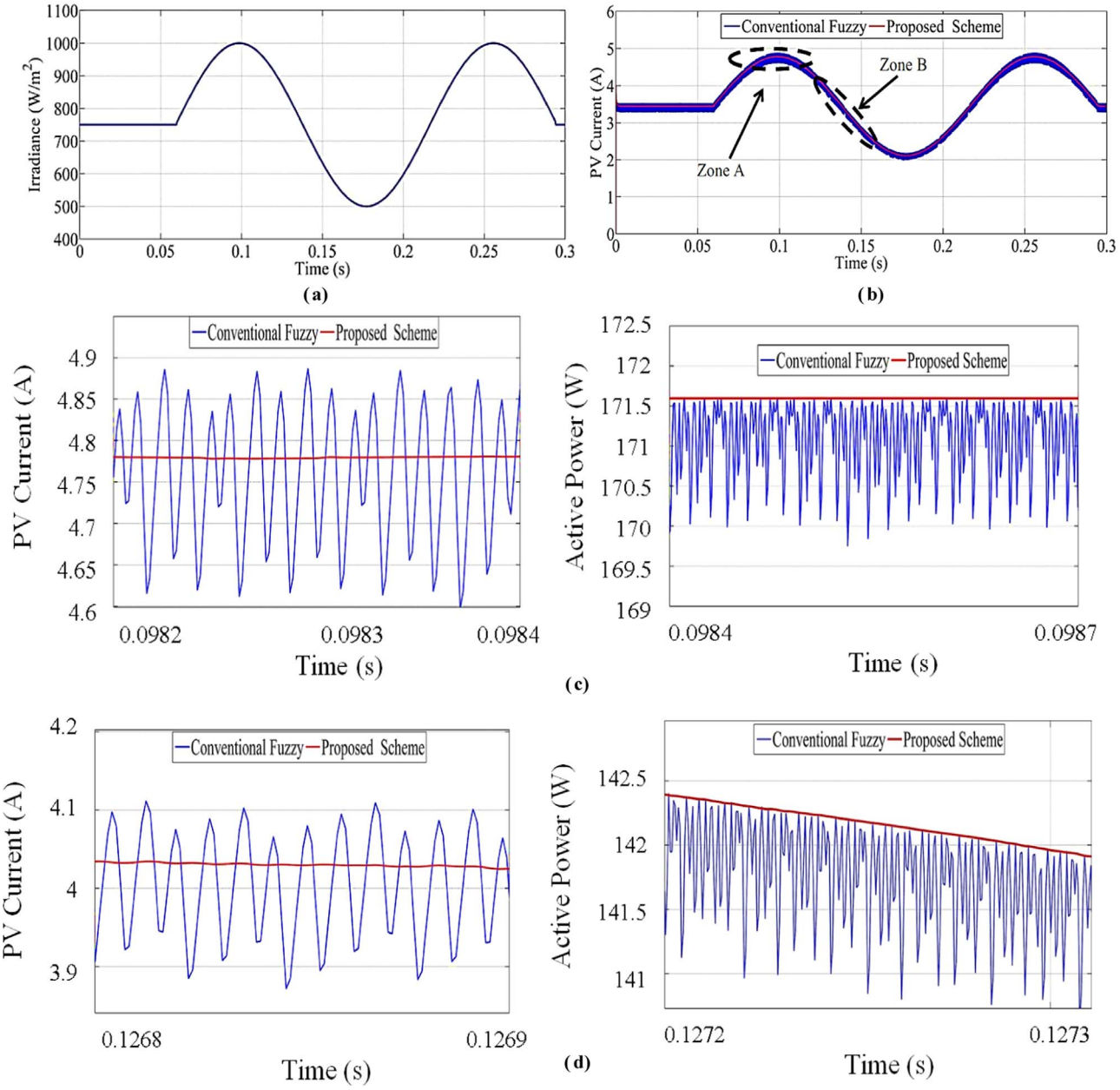

Fig. 6. Sinusoidal Variations test results (a): Applied Irradiance trajectory (b): Sinusoidal Test current tracking (c): Sinusoidal Test results of Zone A (d): Sinusoidal Test results of zone B.

the irradiance level to 1000 W/m^2. As a result of this signal, the irradiance level varies between 500 W/m^2 and 1000 W/m^2 sinosoidally. The test results are demonstrated in Fig. 6.

Similar to the ROPP test, large amounts of current ripples is exhibited by the conventional fuzzy controller's results. Yet, the superiority of the proposed controller is again proven since the current trajectory was tracked with the least amount of oscillations possible by the proposed controller and as a result, negligible active power oscillations are observed.

T.3 One day irradiance and temperature trajectory:

In the third set of simulations, besides variations in irradiance levels, the behavior of controllers considering general variations in the temperature levels throughout one single day are also examined. The utilized data has been collected at a site near Madrid in Spain at March [98]. In this case, by considering the simulation length equivalent to the time interval of the day where sunlight is present, the irradiance level is initially set to its minimum value. As the time passes, this level is increased until it reaches its maximum of S=950 W/m^2. Then, it reduces until the minimum irradiance is reached again at t=18 H. It should be noted that sudden drops and rises in the irradiance level, generally used to model clouds blocking sunlight have also been considered. The applied irradiance and temperature are depicted in Fig. (7a).

As depicted in Fig. (7a) temperature variations follow similar principles. The temperature trajectory initially starts from minimum values, generally modeling early morning conditions. These variations start from the minimum temperature level of 300 K at t=6 H and increase until it reaches T=350 K at t=13 H. Returned to T=310 K at t=18.5 H, the temperature trajectory was designed in a manner so that it exhibits sinusoidal characteristics throughout the simulation time. The behavior of the output current of the PV module in both cases of utilizing conventional FL or the proposed approach is depicted in Fig. (7b).

In Figs. (7c, d) the zoomed plots of the operational behavior of the examined controllers respectively corresponding to Zones A and B are demonstrated. Similar to the ROPP and sinusoidal tests, high magnitudes of oscillations are demonstrated using the conventional direct fuzzy approach. Using the proposed scheme the oscillations in the

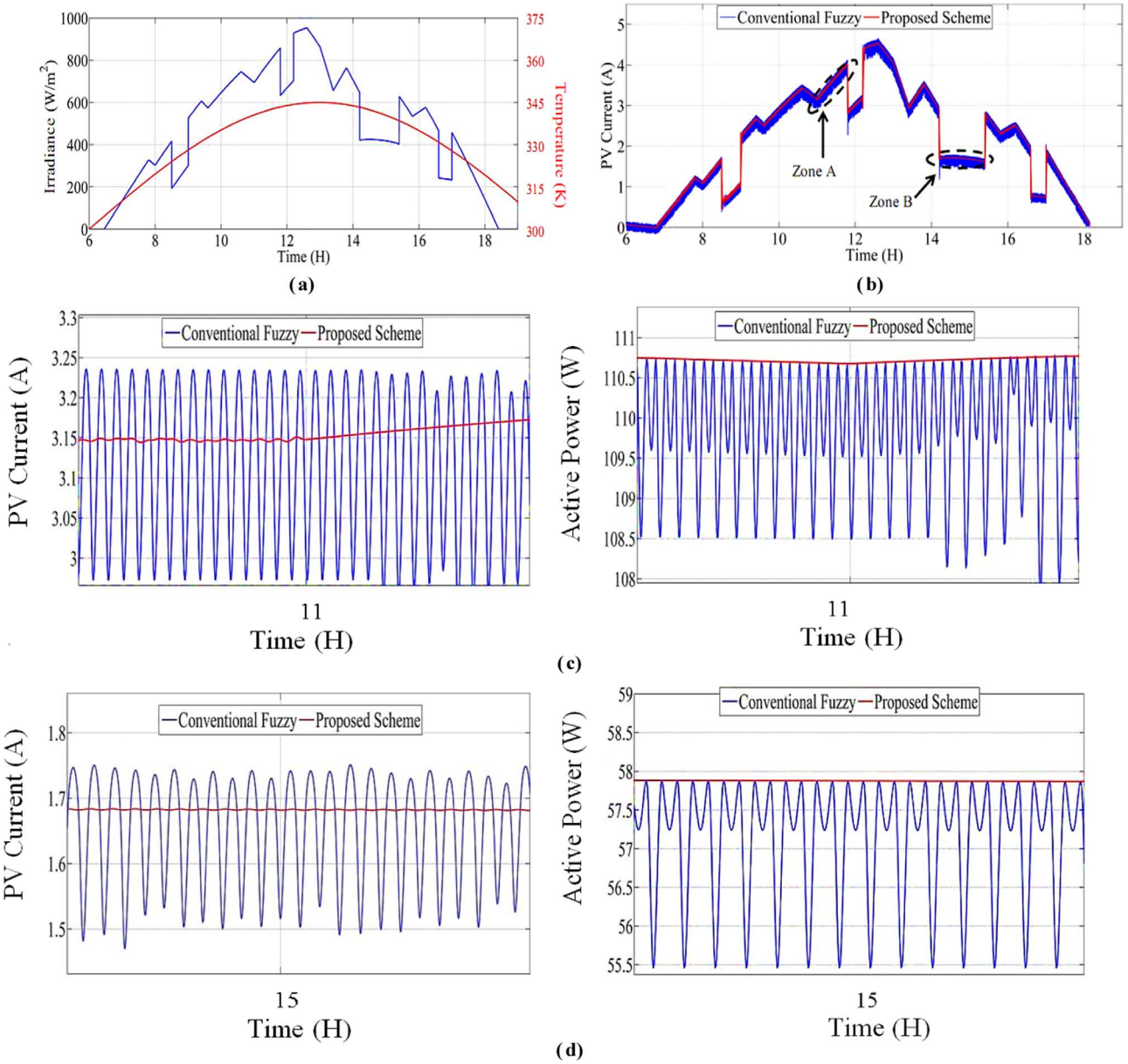

Fig. 7. One Day Irradiance and Temperature Trajectory (a): Applied Temperature and Irradiance Trajectory (b): Output Current r of the PV-Module (c): Output Current and Active Power of the PV-Module Zone A (d): Output Current and Active Power of the PV-Module Zone B.

drawn current are minimized. Diminishing the ripple magnitudes in the drawn current leads to smoother active power from the PV module. These can be confirmed using Figs. (7c, d).

T.4 Tracking reference current performances:

Due to various reasons accurate comparison of the proposed and conventional membership function tuning approaches cannot be accomplished in the performed MPPT tests. Compensation of the effects of inaccurate function estimations using large gains, actuator saturations caused by large control signals and limited over/undershoot due to nonlinear PV-array characteristics could be counted as the main reasons. Therefore, reference tracking performance by the Boost-converter, fed with a fixed input voltage might be a suitable way to directly compare estimation capabilities of the proposed scheme and the conventional approaches such as [37] in tuning continuous functions. In this regard, the reference current signal, as depicted in Fig. 8 was fed to the Boost controller. The control parameters corresponding to this simulation are set to V_{DC}=300 V, $v = 5000_e + I_{MPP}$* and $\hat{\Gamma} = 500$.

The results of this test are depicted in Fig. 8. From Fig. 8 it is evident that the control performance was followed by overshoot/undershoots when using the conventional indirect fuzzy-based approach; while utilizing the proposed scheme, the tracking performance was faster, smoother and with minimum error.

On the other hand, while the conventional indirect fuzzy approach [37] exhibited notable overshoot/undershoots of about (150%, 5% and 10%) respectively at t=[15 ms, 35 ms and 55 ms], no overshoots were observed in the performance of the proposed scheme. Moreover, comparison between rise/settling time of the two controllers in various reference variations are given in Table 12.

As mentioned before, by synchronously tuning the antecedent and consequent membership functions, by exhibiting faster and more accurate tracking, the dynamic performance of the controller has improved. The superior performance of the proposed scheme in dynamic states by reducing the rise/settling time and in steady states by minimizing the tracking error are clearly evident using Table 12 and Fig. 8. As a result of elimination of the overshoots/undershoots, the values for the rise/settling time in the proposed scheme have become equal and have been minimized compared to the scheme presented in [37].

T.5 Generalization of the proposed scheme:

To confirm generalization of the proposed scheme, simulations on other types of PV modules, with the proposed and conventional FL schemes acting as the MPPT controllers were performed. In these simulations, the efforts were put into testing the proposed scheme on different PV modules constructed using different materials. These modules are referred to as multi-junction PV (MJ-PV) modules. In this regard, AIST Nano-crystalline silicon (nc-Si) [100], First Solar, monolithic Cadmium telluride (CdTe) [101] and TEL Solar, Trubbach Labs amorphous silicon/hydrogen alloy with Nano-crystalline silicon alloy (a-Si/nc-Si) [102] PV modules were subjected to test conditions. The corresponding current density as a function of the output voltage

Table 12
Control Comparison Results.

Instance of Reference Variation / Tuning approach		*t=0 ms*	*t=30 ms*	*t=40 ms*	*t=50 ms*	*t=60 ms*
Conventional Approach [37]	Rising time	8 ms	2 ms	3 ms	3 ms	3 ms
	Settling time	22 ms	3 ms	3 ms	11 ms	3 ms
Proposed Approach	Rising time	8 ms	1 ms	2 ms	2 ms	2 ms
	Settling time	8 ms	1 ms	2 ms	2 ms	2 ms.

of these modules is presented in [103]. In this regard, I-V and P-V plots corresponding to a 10 cm×10 cm single PV cell, where $S=1000\ W/m^2$ and $T=300\ K$ are respectively presented in Figs. (9a and b).

As exhibited in Figs. (9a and b) and ref. [103], in these MJ-PV modules, despite acceptable current density, a rather low maximum power is presented. For nc-Si, CdTe and a-Si/nc-Si the expressed maximum powers are 2.2 W, 1.4 W and 1.2 W respectively. To improve the maximum transmittable power so that the modules could be practically implementable in realistic load conditions, for each MJ-PV type, the PV module is considered to be constructed using a combination of 80 cells connected in series. In this regard, the modified I-V and P-V plots corresponding to the modified multi-cell MJPV modules are respectively presented in Figs. (10a and b).

Based on Figs. (10a and b), significant improvements in the maximum transmittable power is observed. The performance of the proposed controller in comparison to the conventional FL was again evaluated in tracking the MPP of the resulting multi-cell MJ-PV modules subjected to irradiance level variations similar to the variations applied in section (V) Fig. (5a). It should be noted that the variations in the overall performance of both examined schemes corresponding to changes in the constructing MJ-PV materials is not considerable and only the magnitudes of steady states and transient oscillations of the conventional FL seem to experience some changes. In this regard, the diagram of the MJ-PV module output "Active Power" is depicted in Fig. 11. In this figure the steady states and dynamic zones are respectively distinguished as "Zone-A" and "Zone-B".

Initially the AIST 11.4% nc-Si [100] is subjected to irradiance variations. Zoomed plots of the active powers are presented in Fig. (12a and b). Similar to the results given in section (V.T1), for the Zone-A results, the proposed scheme followed the MPP with the least error possible while the MJ-PV module controlled by the conventional FL experienced notable power oscillations as expected. Similar results are concluded from Fig. (12b) where the zoomed plot of Zone-B is depicted. As a result, the absolute superiority of the proposed scheme in tracking the MPP over the conventional FL is clearly observable from Fig. 12.

In Figs. (13 and 14) the results of MPPT control applied to First Solar 21% CdTe and Tel Solar 12.2% a-Si/nc-Si are respectively plotted.

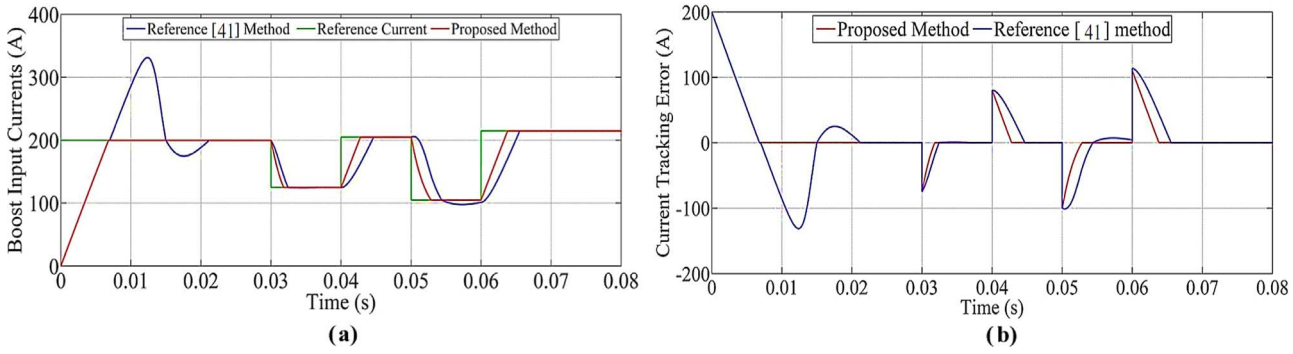

Fig. 8. Reference Tracking Results (a): Current Tracking Performance Test Results (b): Reference Tracking Errors.

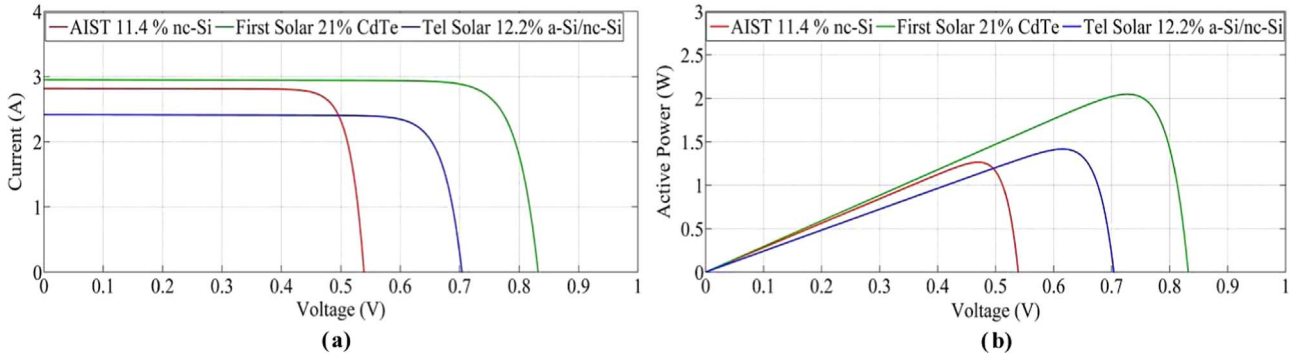

Fig. 9. Output characteristics of various MJ-PV cells (a) I-V plot of various MJ-PV cells (b) P-V plot of various MJ-PV cells.

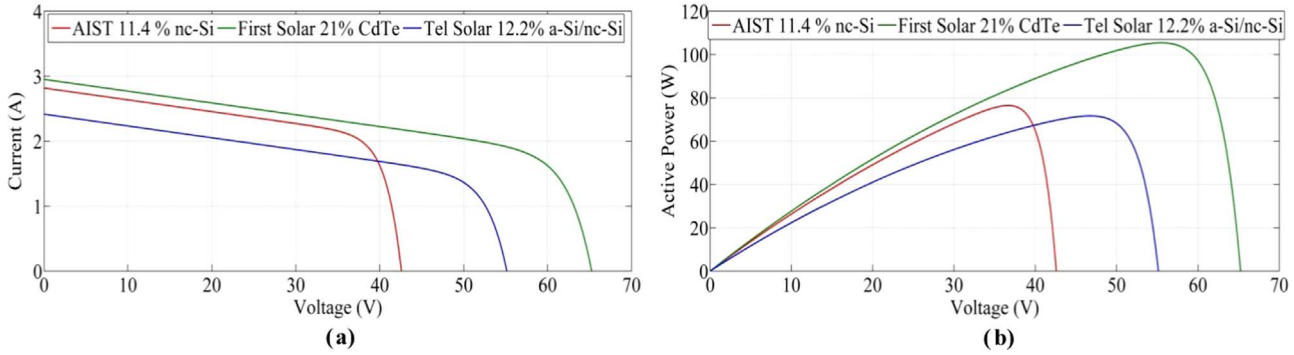

Fig. 10. Output characteristics of various multi-cell MJ-PV cells (a) I-V plot of various multi-cell MJ-PV modules (a) P-V plot of various multi-cell MJ-PV modules.

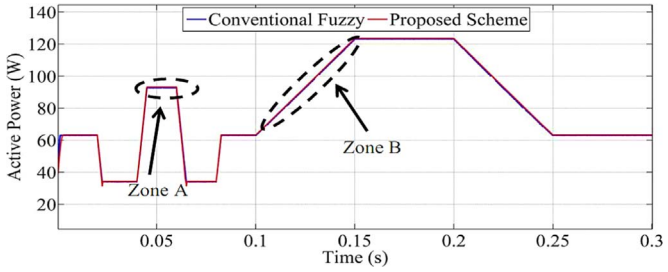

Fig. 11. The MJ-PV module output "Active Power".

The obtained results are similar to the previous results confirming the absolute superiority of the proposed scheme over conventional FL scheme. In this regard, with the MPP being tracked with the minimum error possible, it could be concluded that variations in the structure, materials and formation of the PV module has minimum effect on the performance of the proposed scheme. Based on these conclusions, the proposed scheme can operate desirably in a wide range of PV module types constituted using various types of materials and subjected to various weather conditions (irradiance and temperature variations).

7. Conclusions

A review over conventional MPPT routines is presented in this paper. In this review, after defining minimum MPPT expectations, various MPPT methods were compared in terms of the ability to cover all the defined objectives at the same time. At the end of the review it was concluded that among the available MPPT control methods, only an "antecedent-consequent adaptive" fuzzy based scheme has the potential to fulfill all the design objectives at the same time. Hence, a novel membership functions tuning routine to accomplish optimum MPPT objectives are introduced in this research. On the contrary to available tuning routines, the antecedent and consequent membership functions of the fuzzy-based system are tuned synchronously using a computationally light algorithm. To examine the applicability of the proposed scheme, simulations were performed. In these simulations, the general MPPT field tests, such as the ROPP test, sinusoidal and "one day temperature and irradiance level variation" and the current tracking tests were performed in MATLAB-SIMULINK environment.

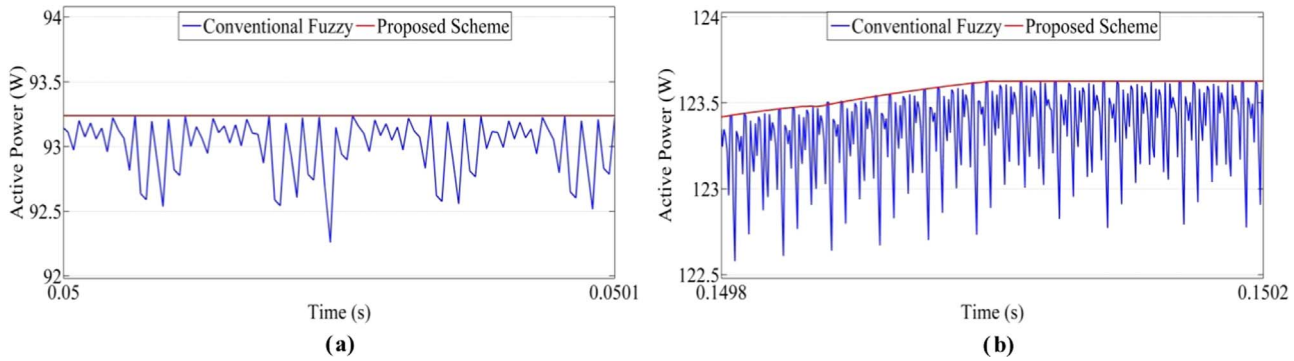

Fig. 12. Active Power plot corresponding to AIST 11.4% nc-Si (a) Active Power plot corresponding to Zone-A of AIST 11.4% nc-Si multi-cell MJ-PV module (b) Active Power plot corresponding to Zone-B of AIST 11.4% nc-Si multi-cell MJ-PV module.

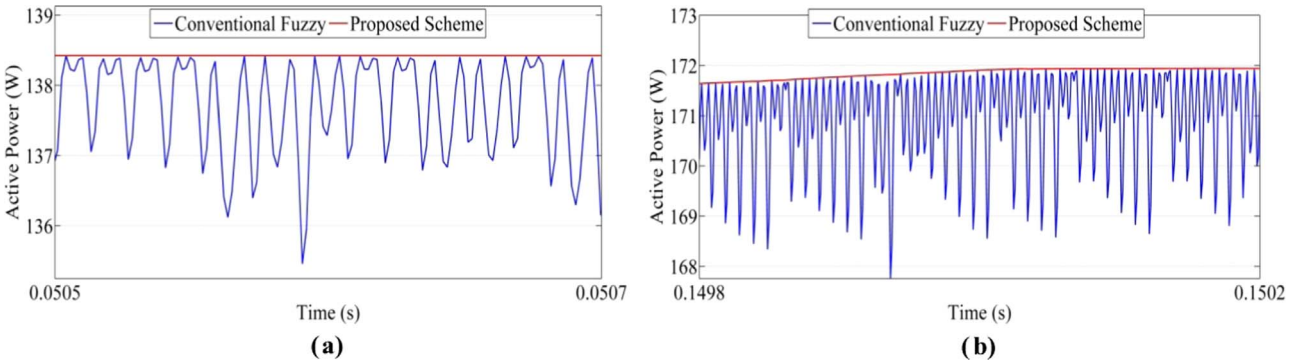

Fig. 13. Active Power plot corresponding to First Solar 21% CdTe (a) Active Power plot corresponding to Zone-A of First Solar 21% CdTe multi-cell MJ-PV module (b) Active Power plot corresponding to Zone-A of First Solar 21% CdTe multi-cell MJ-PV module.

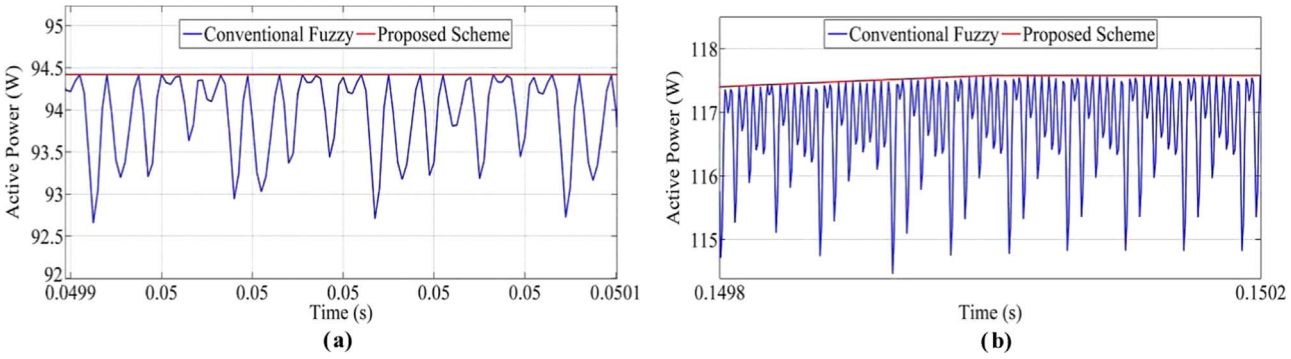

Fig. 14. Active Power plot corresponding to Tel Solar 12.2% a-Si/nc-Si (a) Active Power plot corresponding to Zone-A of Tel Solar 12.2% a-Si/nc-Si multi-cell MJ-PV module (b) Active Power plot corresponding to Zone-A of Tel Solar 12.2% a-Si/nc-Si multi-cell MJ-PV module.

In all the employed tests, the proposed MPPT routine was compared with conventional direct fuzzy MPPT routine. The conventionally tuned adaptive indirect fuzzy-based MPPT routines were also compared with the proposed approach in controlling a reference trajectory. As demonstrated in the simulation results, tuning the antecedent and consequent membership functions improves the tracking performance of the controller, in terms of steady states and dynamic characteristics. As a result, the ripples exhibited by the conventional fuzzy approach in tracking the MPP trajectory were minimized. In this regard, the active power oscillations exhibited by the fuzzy-based schemes were also minimized. Moreover, the dynamic response was also improved compared to the conventionally tuned adaptive fuzzy approach. The results confirm the superiority of the proposed tuning routine in terms of the active power and current oscillations, rising time, settling time and over/undershoots, compared with conventional direct and indirect fuzzy MPPT routines.

References

[1] Wei Haokun, Liu Jian, Yang Biao. Cost-benefit comparison between Domestic Solar Water Heater (DSHW) and Building Integrated Photovoltaic (BIPV) systems for households in urban China. Appl Energy 2014;126:47–55.

[2] Zhang W, Zhu R, Liu B, Ramakrishna S. High-performance hybrid solar cells employing metal-free organic dye modified TiO_2 as photoelectrode. Appl Energy 2012;90:305–8.

[3] Liu Yali, Li Ming, Ji Xu, Luo Xi, Wang Meidi, Zhang Ying. A comparative study of the maximum power point tracking methods for PV system. Energy Convers Manag 2014;85:809–16.

[4] Punitha K, Devaraj D, Sakthivel S. Artificial neural network based modified incremental conductance algorithm for maximum power point tracking in photovoltaic system under partial shading conditions. Energy 2013;62:330–40.

[5] Xiao Xi, Huang Xuanrui, Kang Qing. A hill-climbing-method-based maximum-power-point-tracking strategy for direct-drive wave energy Converters. Ind Electron, IEEE Trans 2016;63(1):257–67.

[6] Al-Amoudi A, Zhang L. Optimal control of a grid-connected PV system for maximum power point tracking and unity power factor. In: Proceedings of the seventh international conference on power electronics and variable speed drives (Conference Publ No. 456);1998 p. 80–5.

[7] Reisi AR, Moradi MH, Jamasb S. Classification and comparison of maximum power point tracking techniques for photovoltaic system: a review. Renew Sustain Energy Rev 2013;19:433–43.

[8] Mellit A, Kalogirou SA. MPPT-based artificial intelligence techniques for photovoltaic systems and its implementation into field programmable gate array chips: review of current status and future perspectives. Energy 2014;70:1–21.

[9] Esram T, Chapman PL. Comparison of photovoltaic array maximum power point tracking techniques. IEEE Trans Energy Convers EC 2007;22(2):439.

[10] Tyugu E. Algorithms and architectures of artificial intelligence. Netherlands: IOS Press; 2007.

[11] Kalogirou SA. Artificial intelligence in energy and renewable energy systems. New York: Nova Science Publisher; 2007.

[12] Cirrincione M, Pucci M, Vitale G. Neural MPPT of variable-pitch wind generators with induction machines in a wide wind speed range. IEEE Trans Ind Appl 2013;49(2):942–53.

[13] Prakash J, Sahoo SK, Karthikeyan SP, Raglend IJ. Design of PSO-Fuzzy MPPT controller for photovoltaic applicationPower Electronics and Renewable Energy Systems. India: Springer; 2015. p. 1339–48.

[14] Daraban S, Petreus D, Morel C. A novel MPPT (maximum power point tracking) algorithm based on a modified genetic algorithm specialized on tracking the global maximum power point in photovoltaic systems affected by partial shading. Energy 2014;74:374–88.

[15] Salah CB, Ouali M. Comparison of fuzzy logic and neural network in maximum power point tracker for PV systems. Electr Power Syst Res 2011;81(1):43–50.

[16] Chekired F, Mellit A, Kalogirou SA, Larbes C. Intelligent maximum power point trackers for photovoltaic applications using FPGA chip: a comparative study. Sol Energy 2014;101:83–99.

[17] Laudani A, Fulginei FR, Salvini A, Lozito GM, and Mancilla-David F. Implementation of a neural MPPT algorithm on a low-cost 8-bit microcontroller. In: Proceedings of international symposium on IEEE power electronics, electrical drives, automation and motion (SPEEDAM); 2014 p. 977–81.

[18] Kofinas P, Dounis AI, Papadakis G, Assimakopoulos MN. An Intelligent MPPT controller based on direct neural control for partially shaded PV system. Energy Build 2015;90:51–64.

[19] Messalti S, Harrag A, Loukriz A. A new variable step size neural networks MPPT controller: review, simulation and hardware implementation. Renew Sustain Energy Rev 2017;68:221–33.

[20] Hafiz F, Abdennour A. An adaptive neuro-fuzzy inertia controller for variable-speed wind turbines. Renew Energy 2016;92:136–46.

[21] Premkumar K, Manikandan BV. Adaptive Neuro-Fuzzy Inference System based speed controller for brushless DC motor. Neurocomputing 2014;138:260–70.

[22] Chaouachi A, Kamel RM, Nagasaka K. A novel multi-model neuro-fuzzy-based MPPT for three-phase grid-connected photovoltaic system. Sol Energy 2010;84(12):2219–29.

[23] Anguera X, Shinozaki T, Wooters C, Hernando J. Model complexity selection and

cross-validation EM training for Robust speaker diarization. In: Proceedings of ICASSP; 2007.
[24] Gao Z, Ming F, Hongling Z. Bagging neural networks for predicting water consumption. J Commun Comput 2005;2(3):19–24, [Serial No. 4].
[25] Yu L, Lai KK, Wang S. Multistage RBF neural network ensemble learning for exchange rates forecasting. Neurocomputing 2008;71(16):3295–302.
[26] Li X, Rakkiyappan R, Balasubramaniam P. Existence and global stability analysis of equilibrium of fuzzy cellular neural networks with time delay in the leakage term under impulsive perturbations. J Frankl Inst 2011;348(2):135–55.
[27] Kuo KY, Lin J. Fuzzy logic control for flexible link robot arm by singular perturbation approach. Appl Soft Comput 2002;2(1):24–38.
[28] Lien CH, Yu KW, Chang HC, Chung LY, Chen JD. Robust reliable guaranteed cost control for uncertain T-S fuzzy neutral systems with interval time-varying delay and linear fractional perturbations. Optim Control Appl Methods 2015;36(1):121–37.
[29] Wang Huanqing, Liu Xiaoping, Liu Peter Xiaoping, Li Shuai. Robust adaptive fuzzy fault-tolerant control for a class of non-lower-triangular nonlinear systems with actuator failures. Inform Sci 2016;336:60–74.
[30] Guenounou Ouahib, Dahhou Boutaib, Chabour Ferhat. Adaptive fuzzy controller based MPPT for photovoltaic systems. Energy Convers Manag 2014;78:843–50.
[31] Eltawil MA, Zhao Z. MPPT techniques for photovoltaic applications. Renew Sustain Energy Rev 2013;25:793–813.
[32] Suganthi L, Iniyan S, Samuel AA. Applications of fuzzy logic in renewable energy systems–a review. Renew Sustain Energy Rev 2015;48:585–607.
[33] Farhat M, Barambones O, Sbita L. Efficiency optimization of a DSP-based standalone PV system using a stable single input fuzzy logic controller. Renew Sustain Energy Rev 2015;49:907–20.
[34] Mendel Jerry M. Uncertain Rule-Based Fuzzy Logic System: Introduction and New Directions. Upper Saddle River, New Jersey: Prentice Hall PTR; 2001.
[35] Boulkroune Abdesselem. A fuzzy adaptive control approach for nonlinear systems with unknown control gain sign. Neurocomputing 2015.
[36] Lin C-K, Wang S-D. Robust self-tuning rotated fuzzy basis function controller for robot arms. IEEE Proc Control Theory Appl 1997;144(4):293–8.
[37] Barkat Said, Tlemçani Abdelhalim, Nouri Hassan. Noninteracting adaptive control of PMSM using interval type-2 fuzzy logic systems. Fuzzy Syst, IEEE Trans 2011;19(5):925–36.
[38] Li HX, Tong S. A hybrid adaptive fuzzy control for a class of nonlinear MIMO systems. Fuzzy Syst, IEEE Trans 2003;11(1):24–34.
[39] Boulkroune Abdesselem, M'saad Mohammed. On the design of observer-based fuzzy adaptive controller for nonlinear systems with unknown control gain sign. Fuzzy Sets Syst 2012;201:71–85.
[40] M.J , Deng C. Online tuning of fuzzy inference systems using dynamic fuzzy Q-learning. Syst, Man, Cybern, Part B: Cybern, IEEE Trans 2004;34(3):1478–89.
[41] Jou JM, Chen PY, Yang SF. An adaptive fuzzy logic controller: its VLSI architecture and applications. Very Large Scale Integr (VLSI) Syst, IEEE Trans 2000;8(1):52–60.
[42] Oh S, Pedrycz W. Identification of fuzzy systems by means of an auto-tuning algorithm and its application to nonlinear systems. Fuzzy Sets Syst 2000;115(2):205–30.
[43] Abu Eldahab YE, Saad NH, Zekry A. Enhancing the maximum power point tracking techniques for photovoltaic systems. Renew Sustain Energy Rev 2014;40:505–14.
[44] Piegari L, Rizzo R. Adaptive perturb and observe algorithm for photovoltaic maximum power point tracking, renewable power generation. IET 2010;4:317–28.
[45] Harrag A, Messalti S. Variable step size modified P & O MPPT algorithm using GA-based hybrid offline/online PID controller. Renew Sustain Energy Rev 2015;49:1247–60.
[46] Mellit A, Kalogirou SA. MPPT-based artificial intelligence techniques for photovoltaic systems and its implementation into field programmable gate array chips: review of current status and future perspectives. Energy 2014;70:1–21.
[47] Ahmed EM, Shoyama M. Variable step size maximum power point tracker using a single variable for stand-alone battery storage PV systems. J Power Electron 2011;11:218–27.
[48] Salas V, Olias E, Lazaro A. Review of the maximum power point tracking algorithms for stand-alone photovoltaic systems. Sol Energy Mater Sol Cells 2006;90:1555–78.
[49] Scarpa V, Buso S, Spiazzi G. Low-complexity MPPT technique exploiting the PV module MPP locus characterization. IEEE Trans Ind Electron 2009;56:1513–38.
[50] Kota VR. Renewable and Sustainable Energy Reviews; 2016, ⟨http://dx.doi.org/10.1016/j.rser.2016.12.054⟩.
[51] Loukriz A, Haddadi M, Messalti S. Simulation and experimental design of a new advanced variable step size incremental conductance MPPT algorithm for PV systems. ISA Trans 2016;62:30–8.
[52] Bahari MI, Tarassodi P, Naeini YM, Khalilabad AK and Shirazi P. Modeling and simulation of hill climbing MPPT algorithm for photovoltaic application. In: Proceedings of IEEE international symposium on power electronics, electrical drives, automation and motion (SPEEDAM); 2016. p. 1041–4.
[53] Miyatake M, Veerachary M, Toriumi F, Fujii N, Ko H. Maximum power point tracking of multiple photovoltaic arrays: a PSO approach. IEEE Trans Aerosp Electron Syst 2011;47(1):367–80.
[54] shaque K, Salam Z, Amjad M, Mekhilef S. An improved particle swarm optimization (PSO)–based MPPT for PV with reduced steady-state oscillation. IEEE Trans Power Electron 2012;27(8):3627–38.
[55] Renaudineau H, Donatantonio F, Fontchastagner J, Petrone G, Spagnuolo G, Martin JP, Pierfederici S. A PSO-based global MPPT technique for distributed PV power generation. IEEE Trans Ind Electron 2015;62(2):1047–58.
[56] Yang H, Zhou W, Lu L, Fang Z. Optimal sizing method for stand-alone hybrid solar–wind system with LPSP technology by using genetic algorithm. Sol Energy 2008;82(4):354–67.
[57] Larbes C, Cheikh SA, Obeidi T, Zerguerras A. Genetic algorithms optimized fuzzy logic control for the maximum power point tracking in photovoltaic system. Renew Energy 2009;34(10):2093–100.
[58] Panda A, Pathak MK, Srivastava SP. Fuzzy intelligent controller for the maximum power point tracking of a photovoltaic module at varying atmospheric conditions. J Energy Technol Policy 2011;1(2):18–27.
[59] Bendib B, Krim F, Belmili H, Almi MF, Boulouma S. Advanced fuzzy MPPT controller for a stand-alone PV system. Energy Procedia 2014;50:383–92.
[60] Chiu CS, Ouyang YL. Robust maximum power tracking control of uncertain photovoltaic systems: a unified TS fuzzy model-based approach. IEEE Trans Control Syst Technol 2011;19(6):1516–26.
[61] El Khateb A, Rahim NA, Selvaraj J, Uddin MN. Fuzzy-logic-controller-based SEPIC converter for maximum power point tracking. IEEE Trans Ind Appl 2014;50(4):2349–58.
[62] Ocran TA, Cao J, Cao B, Sun X. Artificial neural network maximum power point tracker for solar electric vehicle. Tsinghua Sci Technol 2005;10(2):204–8.
[63] Bahgat ABG, Helwa NH, Ahmad GE, El Shenawy ET. Maximum power point traking controller for PV systems using neural networks. Renew Energy 2005;30(8):1257–68.
[64] Ramaprabha R, Mathur BL, Sharanya, M. Solar array modeling and simulation of MPPT using neural network. In: Proceedings of IEEE international conference on control, automation, communication and energy conservation, INCACEC 2009; 2009. p. 1–5.
[65] Kassem AM. MPPT control design and performance improvements of a PV generator powered DC motor-pump system based on artificial neural networks. Int J Electr Power Energy Syst 2012;43(1):90–8.
[66] Kamarzaman NA, Tan CW. A comprehensive review of maximum power point tracking algorithms for photovoltaic systems. Renew Sustain Energy Rev 2014;37:585–98.
[67] Mellit A, Kalogirou SA. MPPT-based artificial intelligence techniques for photovoltaic systems and its implementation into field programmable gate array chips: review of current status and future perspectives. Energy 2014;70:1–21.
[68] Joshi P, Arora S. Maximum power point tracking methodologies for solar PV systems–a review. Renew Sustain Energy Rev 2016.
[69] Kermadi M, Berkouk EM. Artificial intelligence-based maximum power point tracking controllers for photovoltaic systems: comparative study. Renew Sustain Energy Rev 2017;69:369–86.
[70] Messai A, Mellit A, Guessoum A, Kalogirou SA. Maximum power point tracking using a GA optimized fuzzy logic controller and its FPGA implementation. Sol Energy 2011;85(2):265–77.
[71] Ishibuchi H, Yamamoto T. Fuzzy rule selection by multi-objective genetic local search algorithms and rule evaluation measures in data mining. Fuzzy Sets Syst 2004;141(1):59–88.
[72] Castillo L, González A, Pérez R. Including a simplicity criterion in the selection of the best rule in a genetic fuzzy learning algorithm. Fuzzy Sets Syst 2001;120(2):309–21.
[73] Pakhira MK, Bandyopadhyay S, Maulik U. A study of some fuzzy cluster validity indices, genetic clustering and application to pixel classification. Fuzzy Sets Syst 2005;155(2):191–214.
[74] Maulik U, Bandyopadhyay S. Fuzzy partitioning using a real-coded variable-length genetic algorithm for pixel classification. IEEE Trans Geosci Remote Sens 2003;41(5):1075–81.
[75] Kim D, Kim C. Forecasting time series with genetic fuzzy predictor ensemble. IEEE Trans Fuzzy Syst 1997;5(4):523–35.
[76] Alcalá-Fdez J, Alcalá R, Gacto MJ, Herrera F. Learning the membership function contexts for mining fuzzy association rules by using genetic algorithms. Fuzzy Sets Syst 2009;160(7):905–21.
[77] Cheng PC, Peng BR, Liu YH, Cheng YS, Huang JW. Optimization of a fuzzy-logic-control-based MPPT algorithm using the particle swarm optimization technique. Energies 2015;8(6):5338–60.
[78] L10-2:Khaehintung N, Kunakorn A, Sirisuk P. A novel fuzzy logic control technique tuned by particle swarm optimization for maximum power point tracking for a photovoltaic system using a current-mode boost converter with bifurcation control. Int J Control, Autom Syst 2010;8(2):289–300.
[79] Hu Y, Liu J, Liu B. . A MPPT control method of PV system based on fuzzy logic and particle swarm optimization. In: Proceedings of IEEE international conference on intelligent system design and engineering application (ISDEA); 2012. p. 73–5.
[80] Wu H, Sun Y, Meng C. Application of fuzzy controller with particle swarm optimization algorithm to maximum power point tracking of photovoltaic generation system. Proc CSEE 2011;31(6):52–7.
[81] Ibrahim HEA, Elnady MA. A comparative study of PID, fuzzy, fuzzy-PID, PSO-PID, PSO-Fuzzy, and PSO-fuzzy-PID controllers for speed control of DC motor drive. Int Rev Autom Control (IREACO) 2013;6(4):393–403.
[82] Bingül Z, Karahan O. A fuzzy logic controller tuned with PSO for 2 DOF robot trajectory control. Expert Syst Appl 2011;38(1):1017–31.
[83] Bevrani H, Habibi F, Babahajyani P, Watanabe M, Mitani Y. Intelligent frequency control in an AC microgrid: online PSO-based fuzzy tuning approach. IEEE Trans Smart Grid 2012;3(4):1935–44.
[84] Shahzad M, Zahid S, Farooq M. July. A hybrid GA-PSO fuzzy system for user identification on smart phones. In: Proceedings of the 11th annual conference on genetic and evolutionary computation, ACM; 2009. p. 1617–24.
[85] Shayeghi H, Jalili A, Shayanfar HA. Multi-stage fuzzy load frequency control using

PSO. Energy Convers Manag 2008;49(10):2570–80.
[86] Wang LX. Adaptive fuzzy systems and control: design and stability analysis. Upper Saddle River, New Jersey: Prentice-Hall, Inc; 1994.
[87] Hojati M, Gazor S. Hybrid adaptive fuzzy identification and control of nonlinear systems. IEEE Trans Fuzzy Syst 2002;10(2):198–210.
[88] Moradi M, Kazemi MH, Ershadi E. Direct adaptive fuzzy control with membership function tuning. Asian J Control 2012;14(3):726–35.
[89] Hadjili ML, Wertz V. Takagi-Sugeno fuzzy modeling incorporating input variables selection. IEEE Trans Fuzzy Syst 2002;10(6):728–42.
[90] Angelov PP, Filev DP. An approach to online identification of Takagi-Sugeno fuzzy models. IEEE Trans Syst, Man, Cybern, Part B (Cybern) 2004;34(1):484–98.
[91] Oh S, Pedrycz W. Identification of fuzzy systems by means of an auto-tuning algorithm and its application to nonlinear systems. Fuzzy Sets Syst 2000;115(2):205–30.
[92] Qi R, Brdys MA. Stable indirect adaptive control based on discrete-time T–S fuzzy model. Fuzzy Sets Syst 2008;159(8):900–25.
[93] Juang CF, Tsao YW. A self-evolving interval type-2 fuzzy neural network with online structure and parameter learning. IEEE Trans Fuzzy Syst 2008;16(6):1411–24.
[94] Yu W, Li X. Online fuzzy modeling with structure and parameter learning. Exp Syst Appl 2009;36(4):7484–92.
[95] Min YY, Liu YG. Barbalat Lemma and its application in analysis of system stability. J Shandong Univ (Eng Sci) 2007;1:012.
[96] Wang -LX. Adaptive fuzzy systems and control: design and stability analysis. Englewood Cliffs, NJ: Prentice-Hall; 1994.
[97] Chen Chi-Tsong. Linear system theory and design. UK: Oxford University Press, Inc.; 1995.
[98] Mikati M, Santos M, Armenta C. Electric grid dependence on the configuration of a small-scale wind and solar power hybrid system. Renew Energy 2013;57:587–93.
[99] Sharp NE-165U1, Specification sheet, ⟨http://telemetryhelp.com/Datasheets/sharp_165.pdf⟩.
[100] Matsui T, Sai H, Saito K, Kondo M. High-efficiency thin-film silicon solar cells with improved light-soaking stability. Prog Photovolt: Res Appl 2013;21:1363.
[101] First Solar press release, 19 March 2014. First Solar Sets Thin-Film Module Efficiency World Record of 17.0 Percent (⟨http://investor.firstsolar.com/releases.cfm?Sect=all⟩; accessed 24 April ⟨2014⟩).
[102] TEL Solar Press Release, July 9, 2014.
[103] Emery MA, Hishikawa K, Warta, W Y, Dunlop ED. Solar cell efficiency tables (Version 45). Prog Photovolt: Res Appl 2015;23(1):1–9.